

## Determining the usage of the opening space and the impact of single and dual core type walls in multistory buildings subject to seismic loading

Arif Khan, Priyanka Dubey

PG Scholar, CED, Dr. APJ Abdul Kalam University Indore, M.P., India

Assistant Professor, CED, Dr. APJ Abdul Kalam University Indore, M.P., India

**Abstract**—In accordance with the objectives of the research titled "Determination of Usage of Opening Area Effect of Single and Dual Core Type Wall in Multistoried Building Under Seismic Loading," Response Spectrum Analysis was conducted on several building models. These models consisted of 5 single-core buildings with varying shear wall areas: 100% shear wall area (abbreviated as SC1), 90% shear wall area (abbreviated as SC2), 87.5% shear wall area (abbreviated as SC3), and 83.33% shear wall area (abbreviated as SC4). Furthermore, the Response Spectrum Analysis was extended to include six single-core structures with different shear wall areas: 100% (denoted as DC1), 90% (denoted as DC2), 87.5% (denoted as DC3), 83.33% (denoted as DC4), 75% (denoted as DC5), and 50% (denoted as DC6). The seismic impacts of all structural cases were examined, involving seismic shake in both the longitudinal and transverse directions, as required by clause 6.3.3 of IS 1893-2016, to ensure compliance with the specified conditions.

In order to identify the most efficient case, various loads and load combinations were applied to all buildings, and the resulting outcome parameters were compared. The study presents the results in both graphical and tabular formats. The analysis findings, generated using the Staad Pro software, are presented in tabular form alongside multiple graphs with different parameter values. It is important to acknowledge that these research findings provide valuable insights into the effects of opening area in single and dual-core type walls in multistoried buildings under seismic loading. However, further research and validation are required to establish the practical implications of these findings in real-world construction scenarios.

**Keywords**— ETABS, Stability, High Rise Building, single and dual-core, opening space

### I. INTRODUCTION

The issue of vacant and stable land poses a significant challenge in the current construction environment. In urban areas, this scarcity of land has led to an increase in vertical building heights, including low-rise, medium-rise, high-rise, and skyscrapers (above 50 meters tall). However, such structures face vulnerability to lateral and perpendicular stresses, particularly from strong winds and tremors, instead of the more conventional vertical stresses associated with construction. The impact of lateral loads and their potential incongruous proportion to vertical loads becomes a crucial consideration in these situations. Since buildings are designed to primarily handle vertical loads, the lateral loads, which increase rapidly with height, present a different challenge. The lateral load, particularly from wind or seismic activity, generates an enormous overturning moment at the base of the structure, which varies with the square of the building's height. As the lateral loads tend to be higher at the topmost stories compared to the bottom, the building may behave as a cantilever, experiencing swaying due to these sideways lateral stresses. Buildings that were not designed to withstand these seismic loads have shown vulnerability, leading to collapses in seismically active regions. Therefore, it is crucial to thoroughly investigate the causes and effects of lateral loads and consider them in the construction process. One essential structural element used to counter earthquake forces or equivalent forces within the plane of a wall is a shear wall. Shear walls are commonly incorporated into tall buildings to prevent total structural failure due to seismic loads. In conclusion, the challenges posed by vacant land and the need for taller buildings require a comprehensive understanding of lateral loads and their impact on construction. By incorporating appropriate measures, such as shear walls, buildings can be better equipped to withstand seismic forces and ensure safety in seismically active regions.

### OBJECTIVE

The Staad Pro model was used in this multistory building study to determine the influence of single and dual core type walls on opening areas in multistory buildings subject to seismic loading. There are a total of 11 instances of multistory buildings in earthquake zone III with medium soil conditions. In both longitudinal and

transverse directions, results are examined for stresses, displacements, base shear, etc. The most effective floor level will then be optimized..

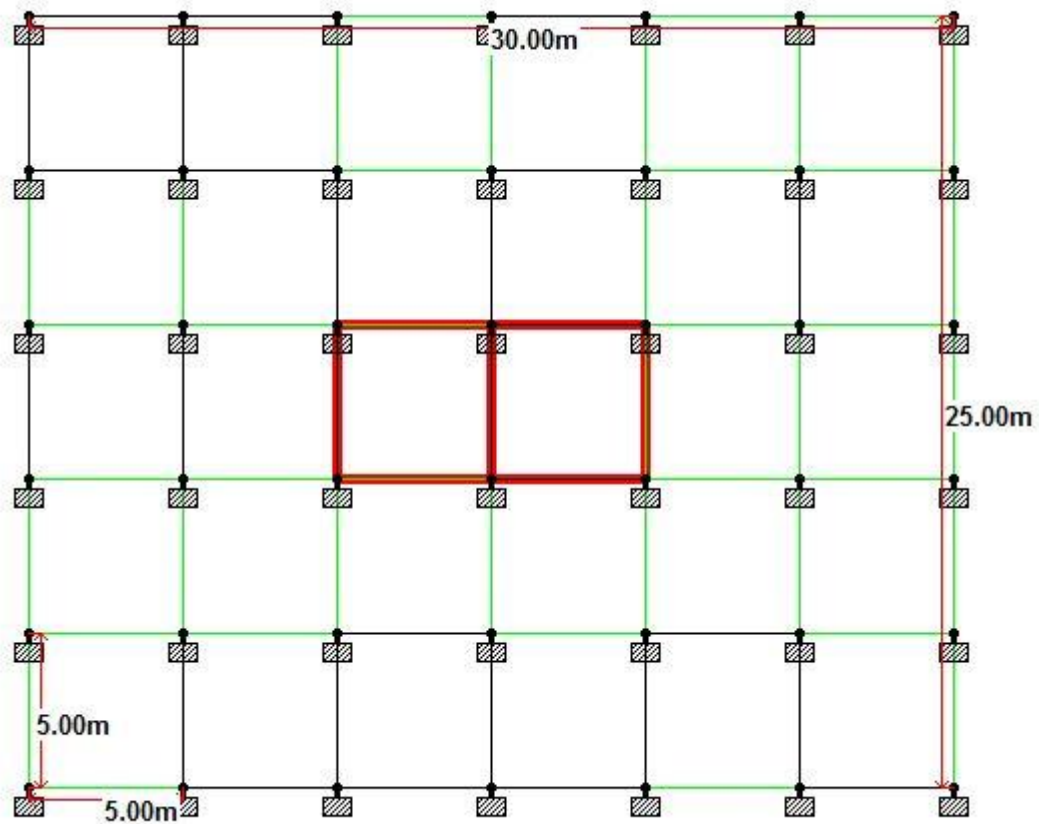


Fig 1 Plan of the building single core

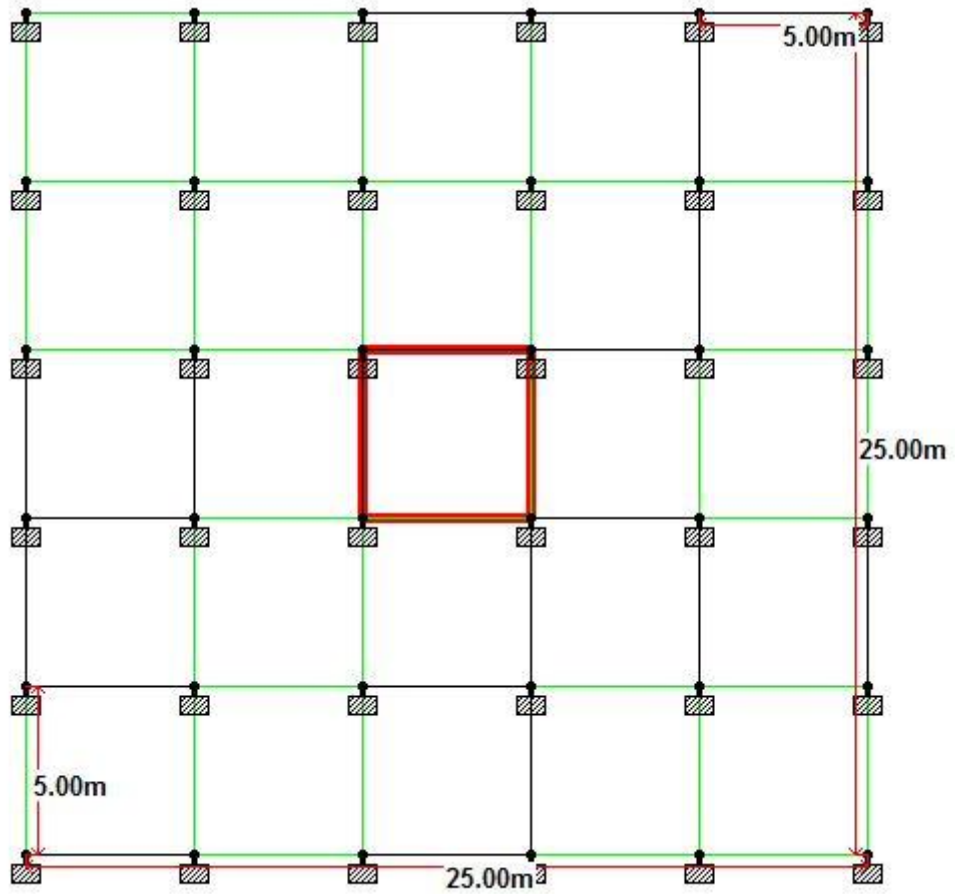


Fig 2 Plan of the building dual core

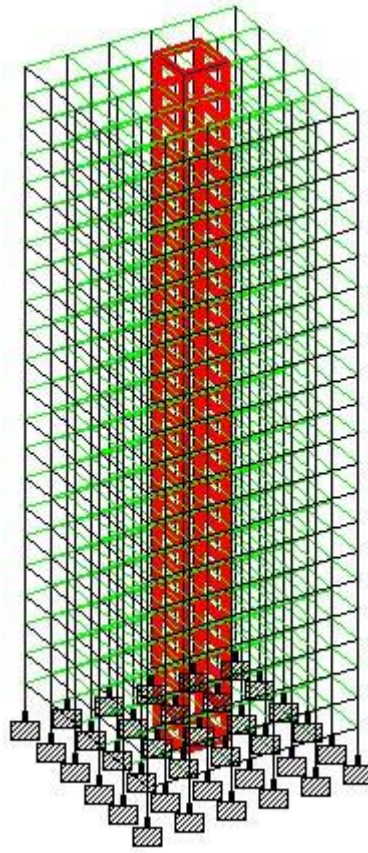


Fig 3 Elevation of the building single core

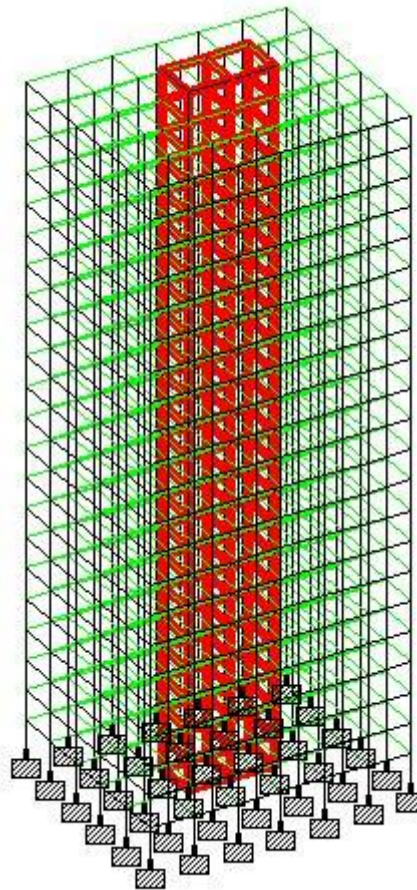


Fig 4 Elevation of the building dual core

Building configuration	G+20
No. of bays in X direction	6
No. of bays in Z direction	5
Height of building	73.5 M
Dimensions of building	25M X 25M(single core) 30M X 25M(dual core)
Size of beam	0.45 X 0.60
Size of column	0.55 X 0.65
Concrete and Steel Grade	M 30 & FE415

Table 1 Details of building

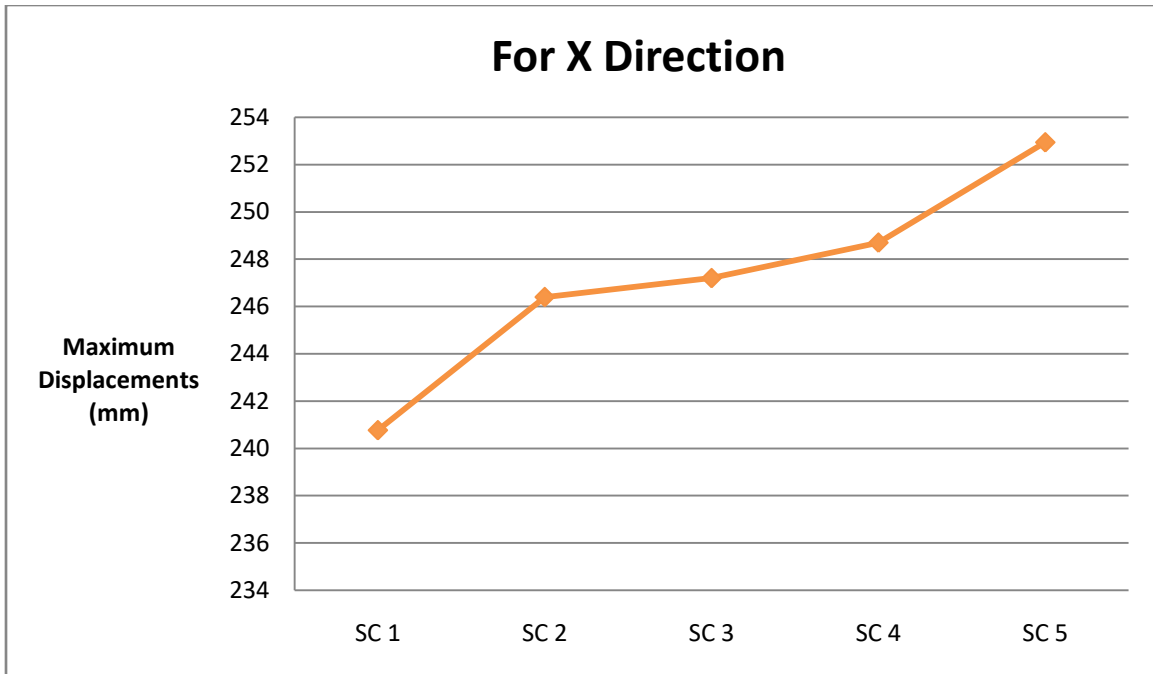
Earthquake parameters	Zone III with RF 4 & 5% damping ratio
Period in X & Z direction	1.0655 & 1.0655 for both direction
Dead load for floor with waterproofing	1.2KN/m <sup>2</sup>
Live load for floor and roof	4KN/M <sup>2</sup> & 1KN/M <sup>2</sup>

Table 2 Detail of loading

**II. RESULT AND DISCUSSION**

**Table 4.89:** Maximum Displacement in X direction for all Single Core Cases

Single Core Case	Maximum Displacement (mm)
	For X Direction
SC 1	240.77
SC 2	246.4
SC 3	247.2
SC 4	248.7
SC 5	252.94



**Fig. 4.1:** Graphical Representation of Maximum Displacement in X direction for all Single Core Cases

**Table 4.90:** Maximum Displacement in Z direction for all Single Core Cases

Single Core Case	Maximum Displacement (mm)
	For Z Direction
SC 1	249.68
SC 2	255.57
SC 3	256.46
SC 4	258.09
SC 5	265.94

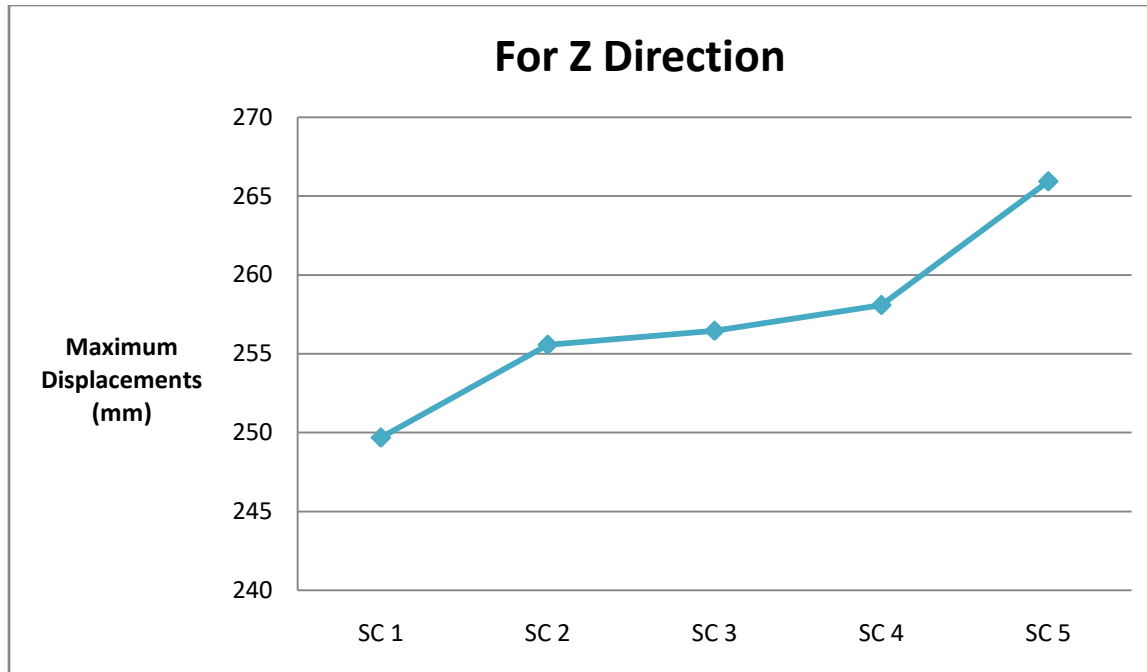


**Fig. 4.2:** Graphical Representation of Maximum Displacement in Z direction for all Single Core Cases

**Table 4.91:** Storey Drift in X direction for all Single Core Cases

S. No.	Height (m)	Storey Drift (cm)				
		For X Direction				
		SC 1	SC 2	SC 3	SC 4	SC 5
1	0	0	0	0	0	0
2	3.5	0.2266	0.3596	0.3941	0.4623	0.648
3	7	0.4577	0.6145	0.6457	0.7076	0.876
4	10.5	0.6353	0.7642	0.7884	0.8358	0.9675
5	14	0.7848	0.8931	0.913	0.9523	1.0661
6	17.5	0.9069	0.9983	1.0152	1.0542	1.1464
7	21	1.0051	1.0828	1.0973	1.1312	1.2183
8	24.5	1.0821	1.1485	1.1611	1.1902	1.2603
9	28	1.1405	1.1975	1.2087	1.2333	1.2962
10	31.5	1.1821	1.2312	1.2412	1.2621	1.3193
11	35	1.2086	1.2511	1.2601	1.2777	1.3297



12	38.5	1.2215	1.2582	1.2664	1.2821	1.3293
13	42	1.222	1.2536	1.2609	1.275	1.3171
14	45.5	1.2115	1.2382	1.2447	1.2571	1.2941
15	49	1.191	1.2131	1.2187	1.2293	1.2606
16	52.5	1.1619	1.1793	1.1838	1.1922	1.2172
17	56	1.1256	1.1381	1.1411	1.147	1.1645
18	59.5	1.0838	1.0907	1.0921	1.0947	1.1033
19	63	1.0383	1.0389	1.0383	1.037	1.035
20	66.5	0.9913	0.9849	0.9818	0.9758	0.9616
21	70	0.946	0.9315	0.9257	0.9145	0.8871
22	73.5	0.9076	0.8827	0.8743	0.8583	0.8181
23	77	0.8414	0.8297	0.8181	0.796	0.7484
24	80.5	0.9119	0.8838	0.8769	0.8526	0.819

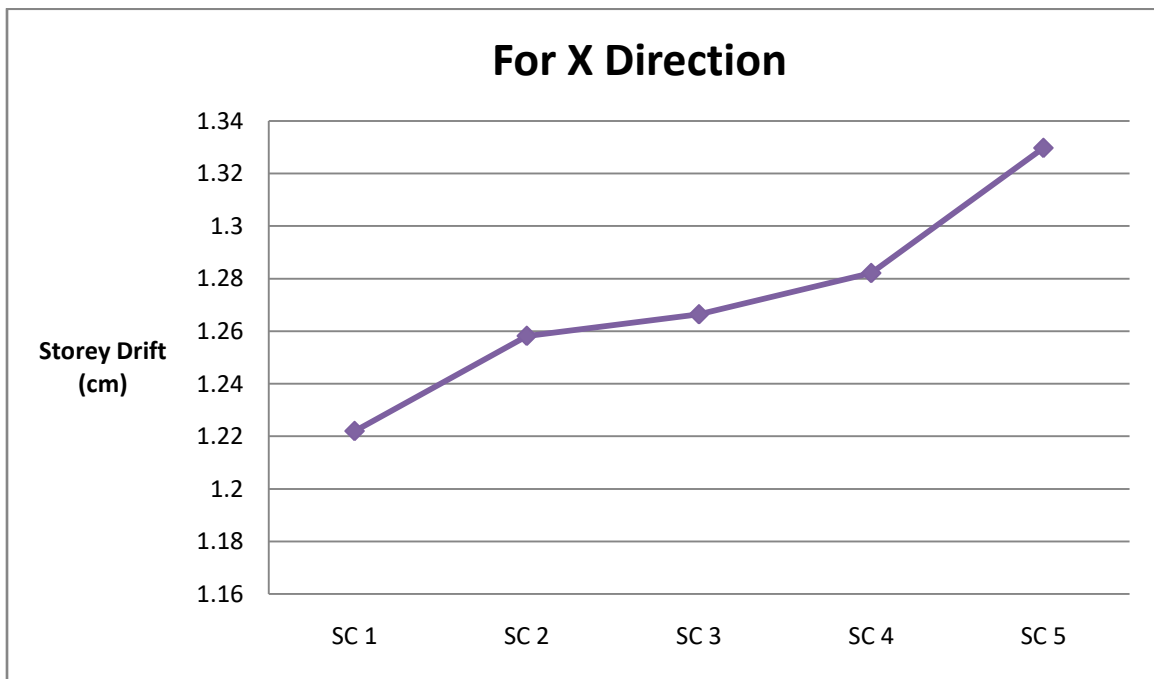
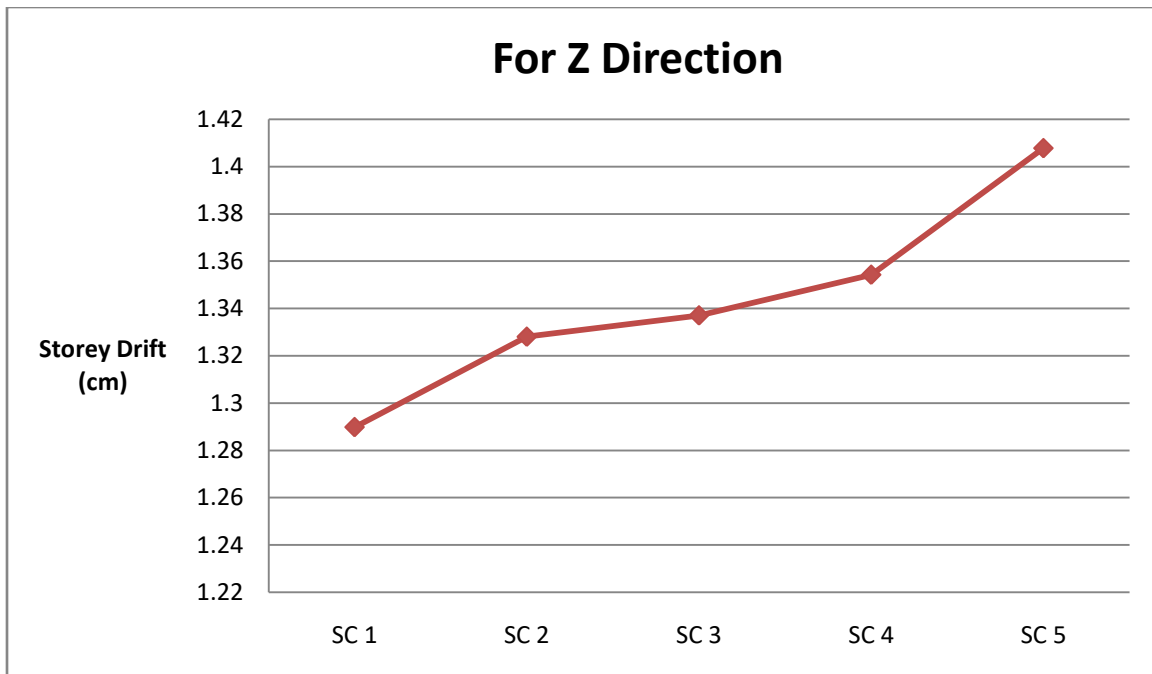


Fig. 4.3: Graphical Representation of Storey Drift in X direction for all Single Core Cases

**Table 4.92:** Storey Drift in Z direction for all Single Core Cases

S. No.	Height (m)	Storey Drift (cm)				
		For Z Direction				
		SC 1	SC 2	SC 3	SC 4	SC 5
1	0	0	0	0	0	0
2	3.5	0.2357	0.3312	0.3449	0.4952	0.7106
3	7	0.4736	0.6206	0.6413	0.7383	0.9223
4	10.5	0.6614	0.7979	0.8214	0.874	1.0181
5	14	0.8194	0.9378	0.9596	0.9982	1.123
6	17.5	0.9489	1.0501	1.0695	1.1071	1.2154
7	21	1.0534	1.14	1.1569	1.1898	1.2777
8	24.5	1.1359	1.21	1.2248	1.2534	1.3312
9	28	1.1988	1.2623	1.2753	1.3132	1.3753
10	31.5	1.244	1.2985	1.3099	1.3317	1.3976
11	35	1.2733	1.32	1.3302	1.3492	1.4078
12	38.5	1.2881	1.3281	1.3371	1.3543	1.4073
13	42	1.2899	1.3239	1.3317	1.3477	1.3949
14	45.5	1.28	1.3083	1.315	1.3296	1.371
15	49	1.2596	1.2826	1.288	1.301	1.3359
16	52.5	1.2302	1.2477	1.2518	1.2626	1.2904
17	56	1.1933	1.2051	1.2075	1.2157	1.2352
18	59.5	1.1505	1.1561	1.1566	1.1616	1.1711
19	63	1.1039	1.1026	1.1008	1.1017	1.0994
20	66.5	1.0559	1.0469	1.0424	1.0384	1.0229
21	70	1.0096	0.992	0.9845	0.9751	0.9452
22	73.5	0.9705	0.9421	0.9319	0.9176	0.874
23	77	0.9049	0.8887	0.8749	0.8566	0.8036
24	80.5	0.9744	0.9418	0.9324	0.9215	0.8746



**Fig. 4.4:** Graphical Representation of Storey Drift in Z direction for all Single Core Cases

**Table 4.93:** Base Shear in X and Z direction for all Single Core Cases

Single Core Case	Base Shear (KN)	
	X direction	Z direction
SC 1	12710.04	12532.19
SC 2	12294.27	12116.86
SC 3	12192.59	12012.74
SC 4	11997.09	11813.33
SC 5	11477.37	11275.85

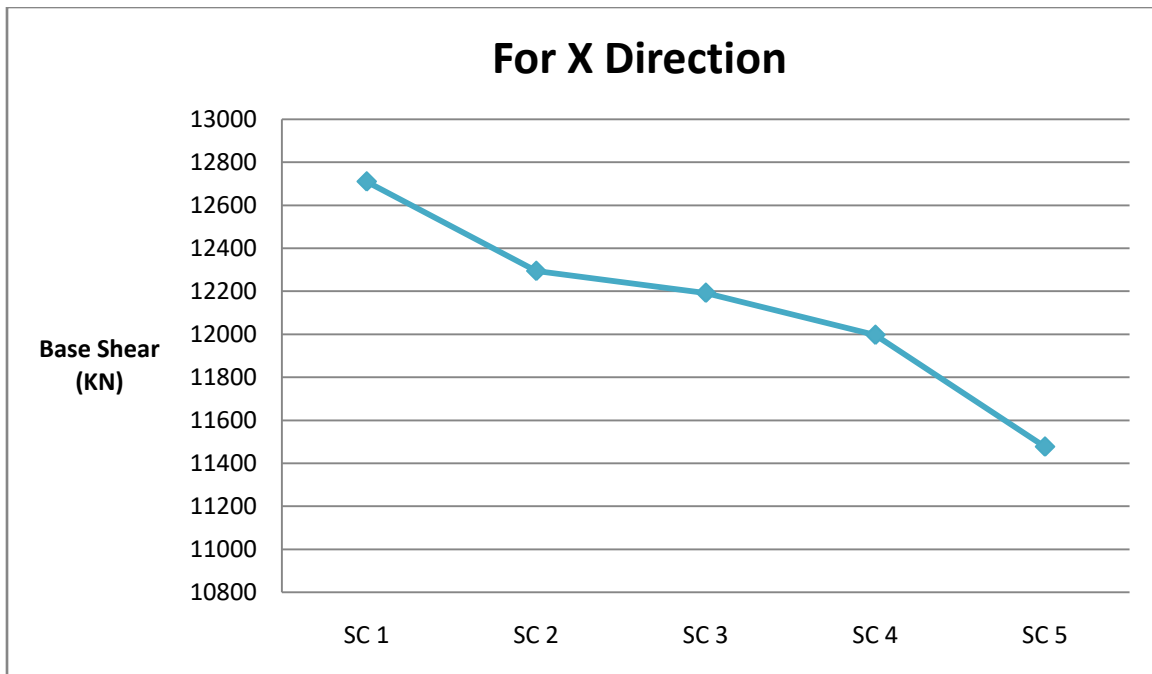


**Fig. 4.5:** Graphical Representation of Base Shear in X direction for all Single Core Cases

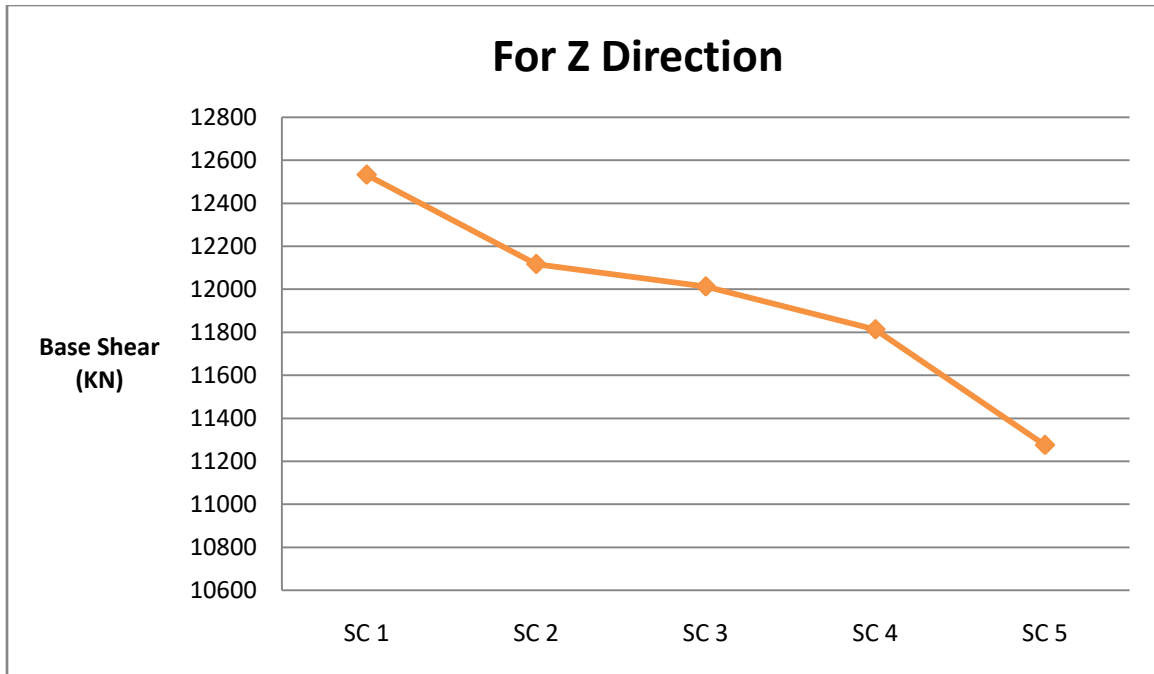


**Fig. 4.6:** Graphical Representation of Base Shear in Z direction for all Single Core Cases

**Table 4.94:** Time Period and Mass Participation Factor for all Single Core Cases

Single Core Case	Time Period (Seconds)	Participation X %	Time Period (Seconds)	Participation Z %
SC 1	3.568	70.553	3.66	70.373
SC 2	3.69	72.408	3.787	72.274
SC 3	3.713	72.755	3.812	72.631
SC 4	3.757	73.392	3.859	73.291
SC 5	3.882	74.953	3.994	74.931

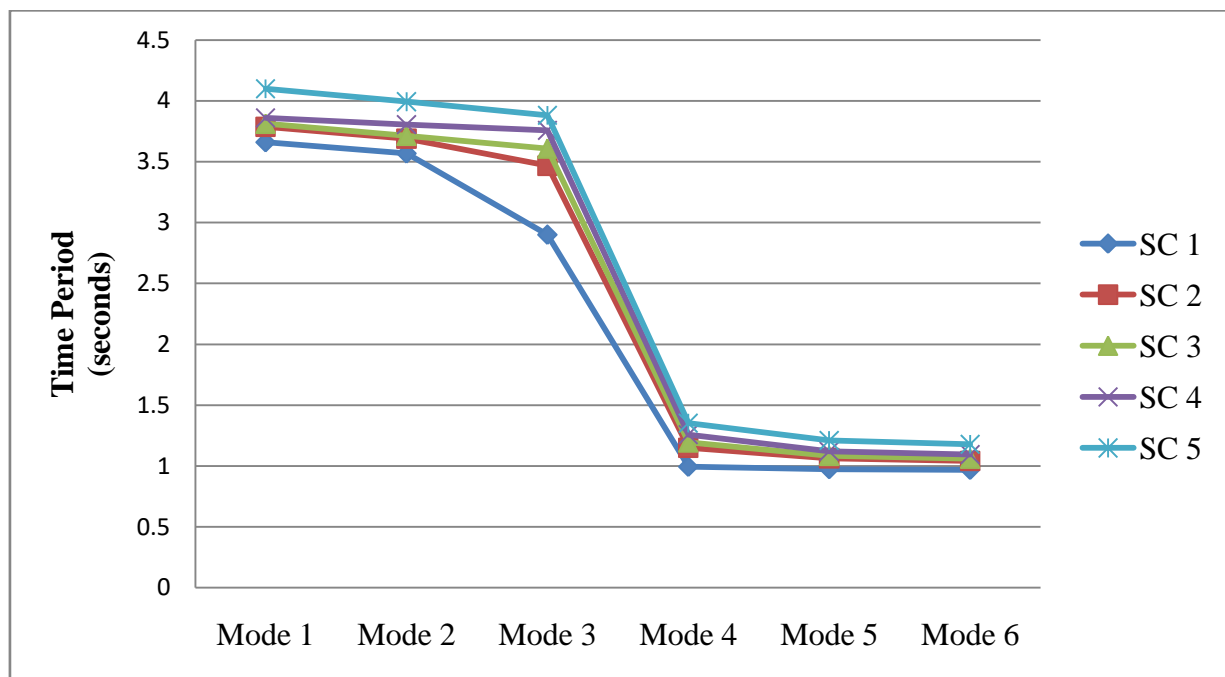


**Fig. 4.7:** Graphical Representation of Time Period Time Period for all Single Core Cases

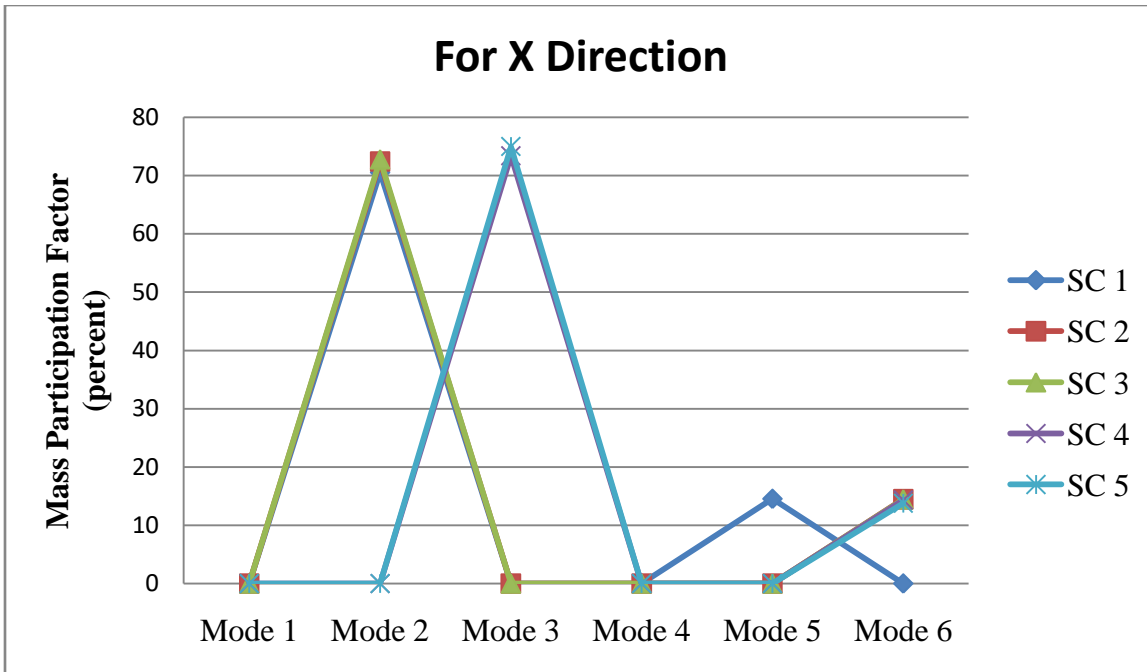


**Fig. 4.8:** Graphical Representation of Mass Participation Factor in X direction for all Single Core Cases

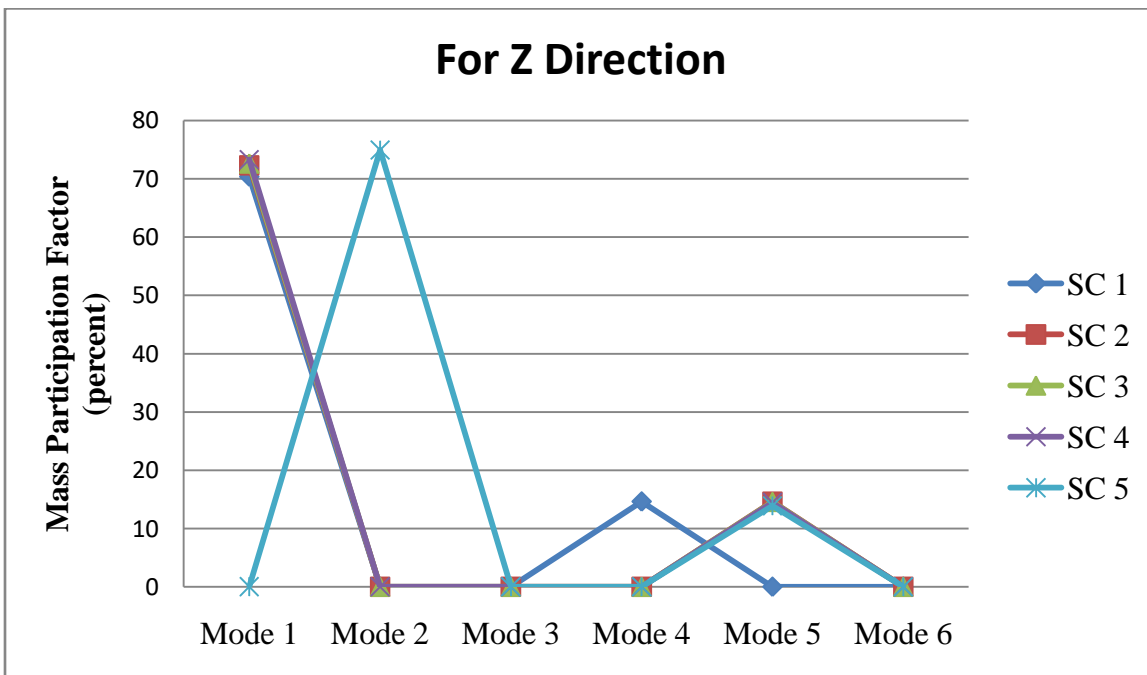


**Fig. 4.9:** Graphical Representation of Mass Participation Factor in Z direction for all Single Core Cases

**Table 4.95:**Maximum Axial Forces in Column for all Single Core Cases

Single Core Case	Column Axial Force (KN)
SC 1	10336.457
SC 2	14518.827
SC 3	14365.37
SC 4	14077.065
SC 5	13369.7

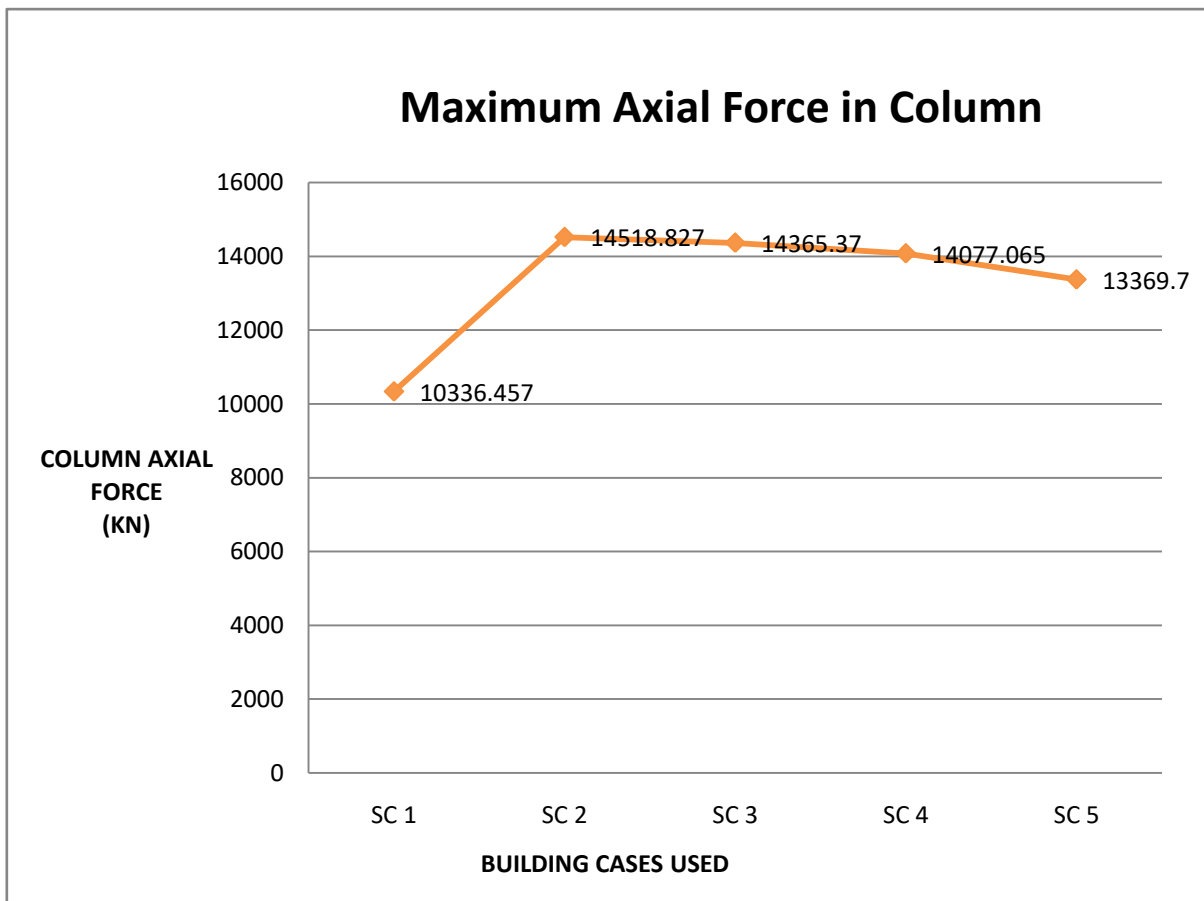


**Fig. 4.10:** Graphical Representation of Maximum Axial Forces in Column for all Single Core Cases



**Table 4.96:** Maximum Shear Forces in Columns for all Single Core Cases

Single Core Case	Column Shear Force (KN)	
	Shear along Y	Shear along Z
SC 1	316.628	297.044
SC 2	303.025	290.389
SC 3	302.566	290.021
SC 4	301.878	289.515
SC 5	301.488	289.622

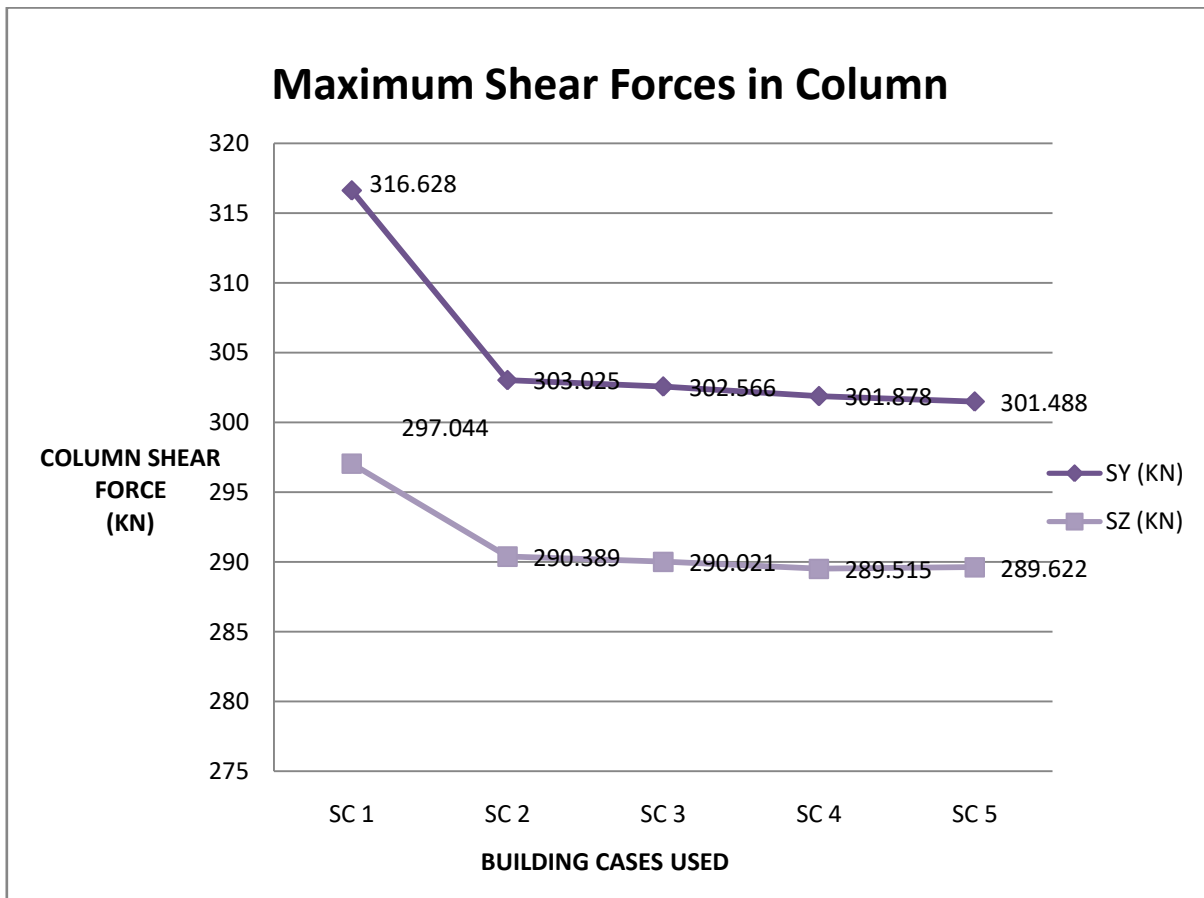


**Fig. 4.11:** Graphical Representation of Maximum Shear Forces in Columns for all Single Core Cases

**Table 4.97:** Maximum Bending Moment in Columns for all Single Core Cases

Single Core Case	Column Bending Moment (KNm)	
	Moment along Y	Moment along Z
SC 1	575.994	626.13
SC 2	538.57	584.465
SC 3	530.565	575.653
SC 4	515.762	559.403
SC 5	507.841	529.022

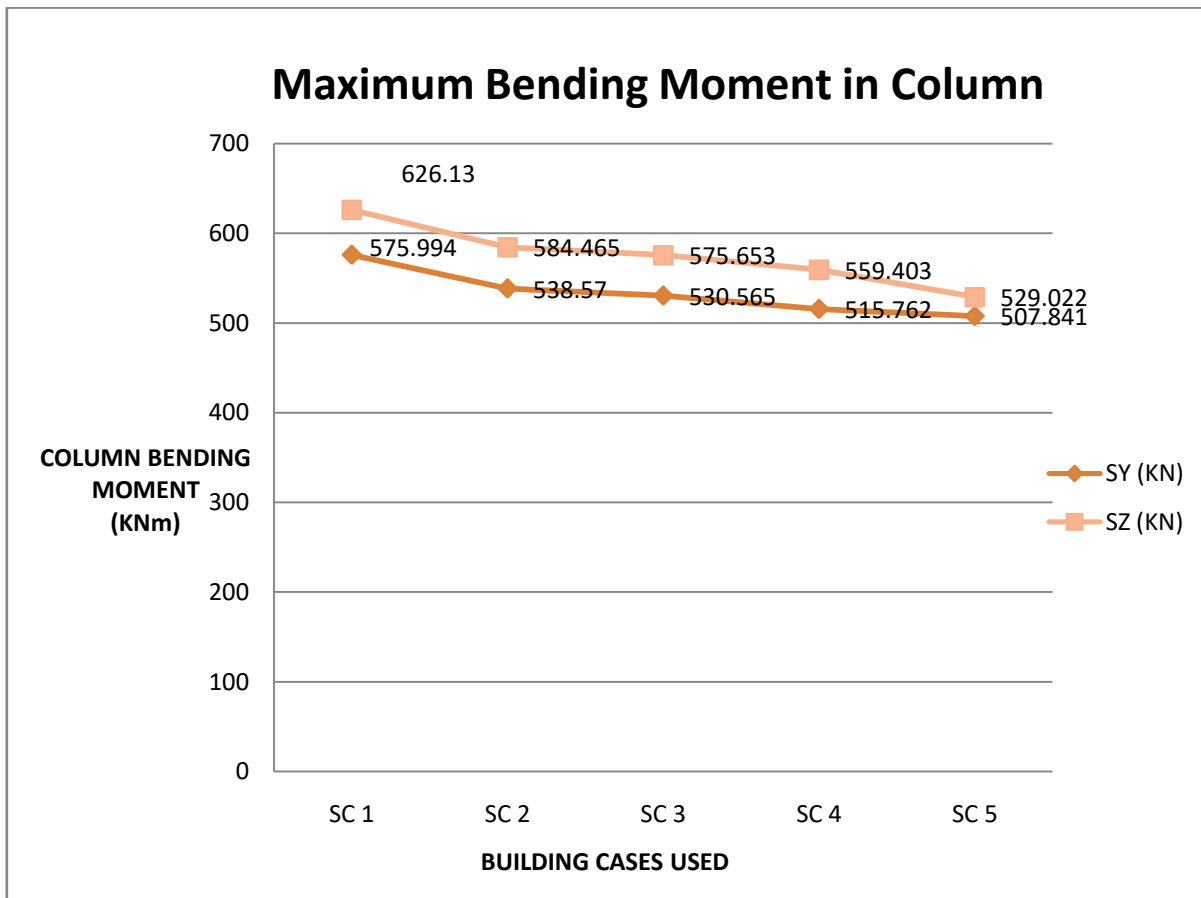


**Fig. 4.12:** Graphical Representation of Maximum Bending Moment in Columns for all Single Core Cases

**Table 4.98:** Maximum Shear Forces in beams parallel to X direction for all Single Core Cases

Single Core Case	Beam Shear Force (parallel to X direction) (KN)
SC 1	261.029
SC 2	3197.668
SC 3	3062.74
SC 4	2812.972
SC 5	2459.933

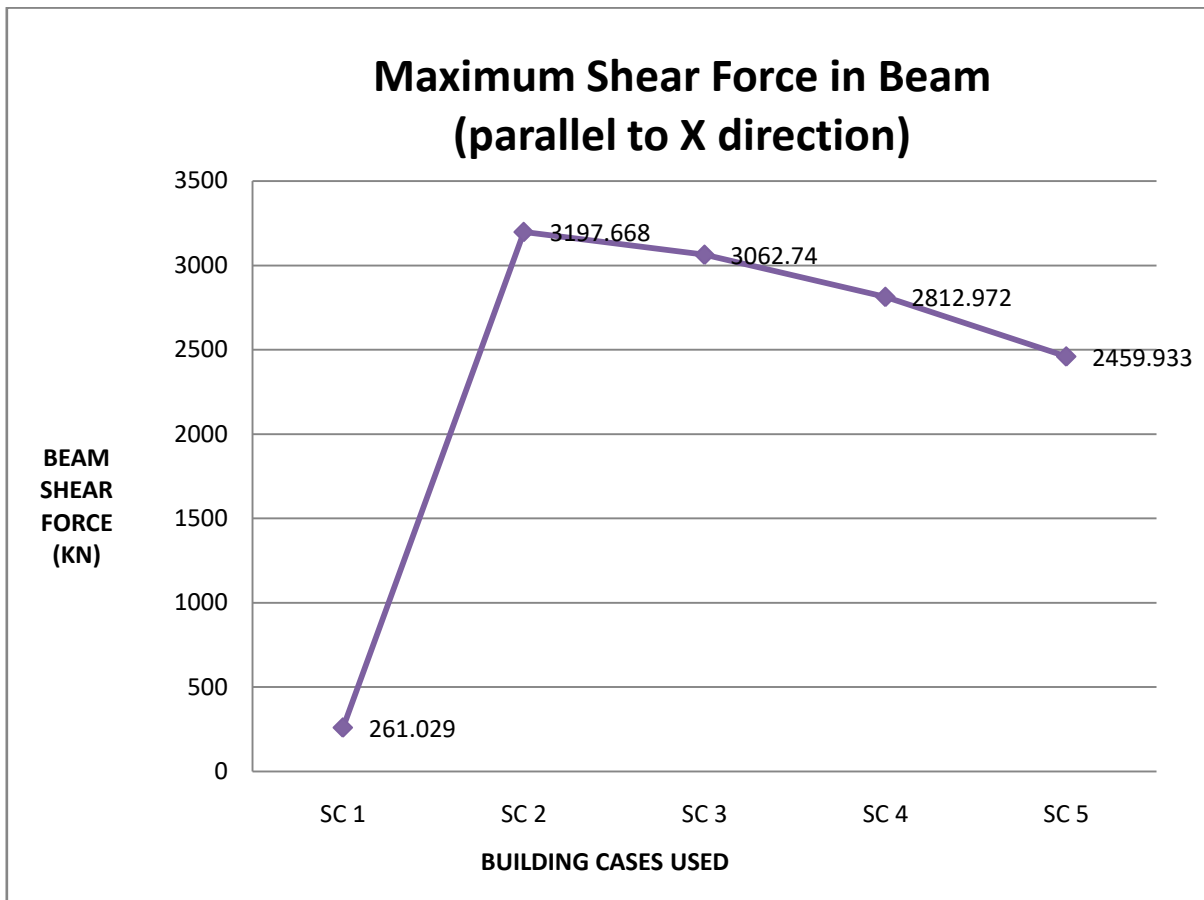


**Fig. 4.13:** Graphical Representation of Maximum Shear Forces in beams parallel to X direction for all Single Core Cases

**Table 4.99:** Maximum Shear Forces in beams parallel to Z direction for all Single Core Cases

Single Core Case	Beam Shear Force (parallel to Z direction) (KN)
SC 1	259.687
SC 2	3244.98
SC 3	3114.367
SC 4	2910.902
SC 5	2617.457

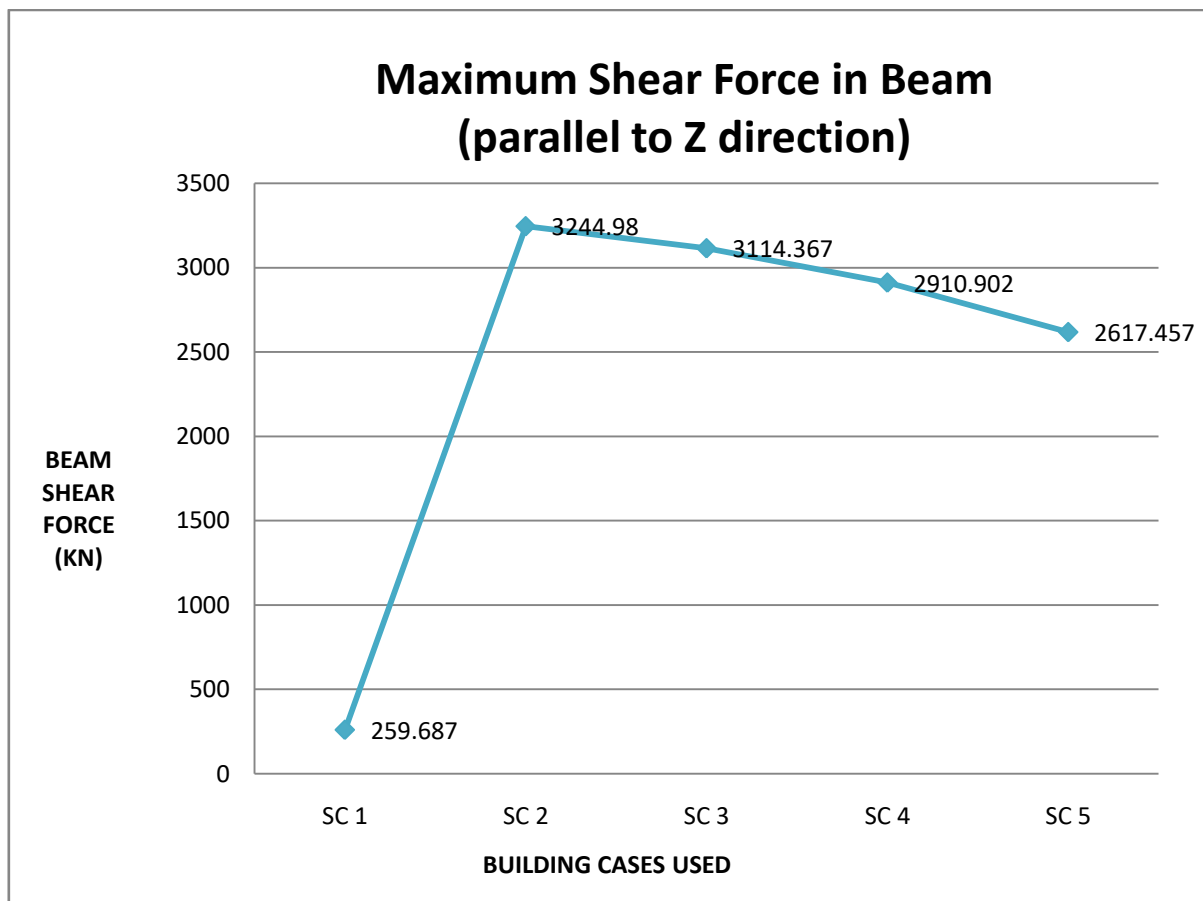


**Fig. 4.14:** Graphical Representation of Maximum Shear Forces in beams parallel to Z direction for all Single Core Cases

**Table 4.100:** Maximum Bending Moment in beams parallel to X direction for all Single Core Cases

Single Core Case	Beam Bending Moment (along X direction) (KNm)
SC 1	548.313
SC 2	799.652
SC 3	957.279
SC 4	1183.928
SC 5	1566.24

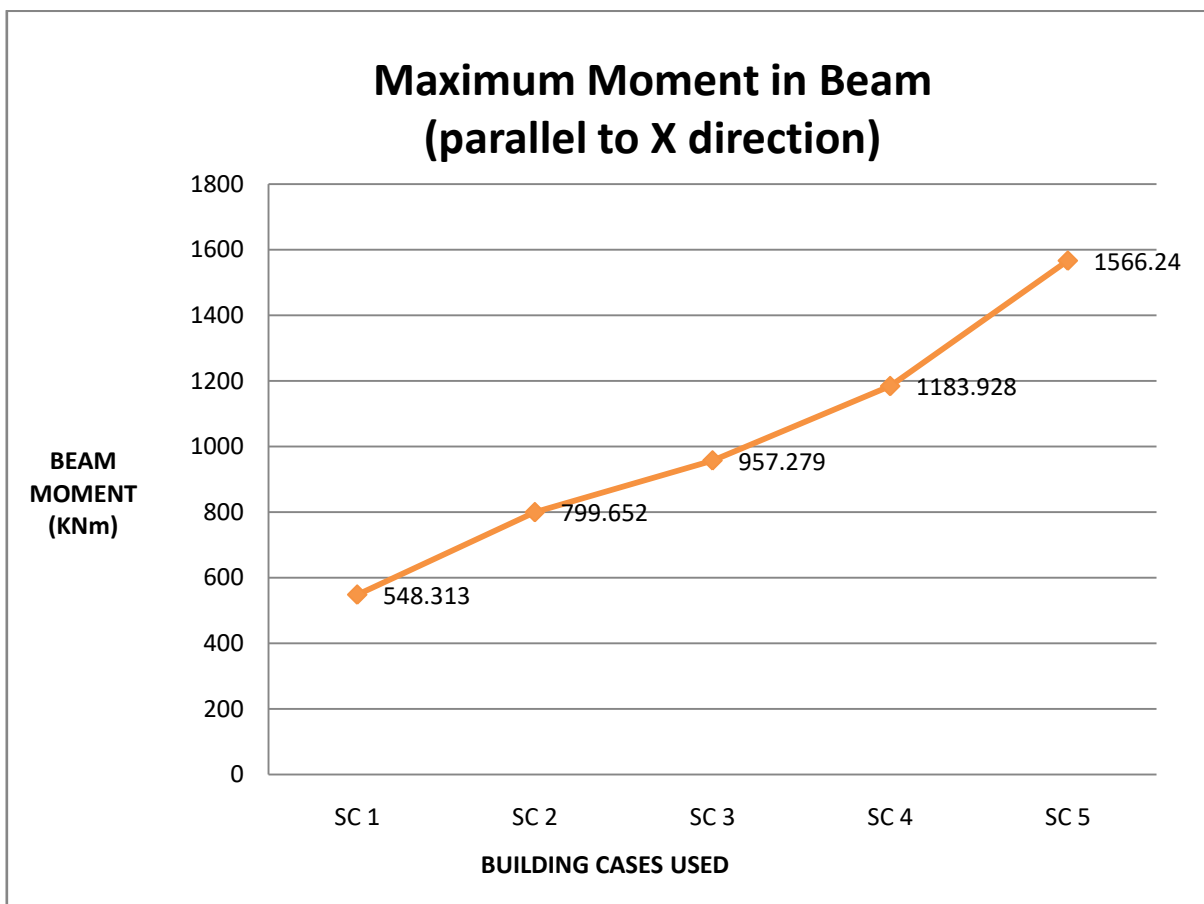


**Fig. 4.15:** Graphical Representation of Maximum Bending Moment in beams parallel to X direction for all Single Core Cases

**Table 4.101:** Maximum Bending Moment in beams parallel to Z direction for all Single Core Cases

Single Core Case	Beam Bending Moment (along Z direction) (KNm)
SC 1	550.358
SC 2	820.361
SC 3	990.118
SC 4	1234.774
SC 5	1658.24

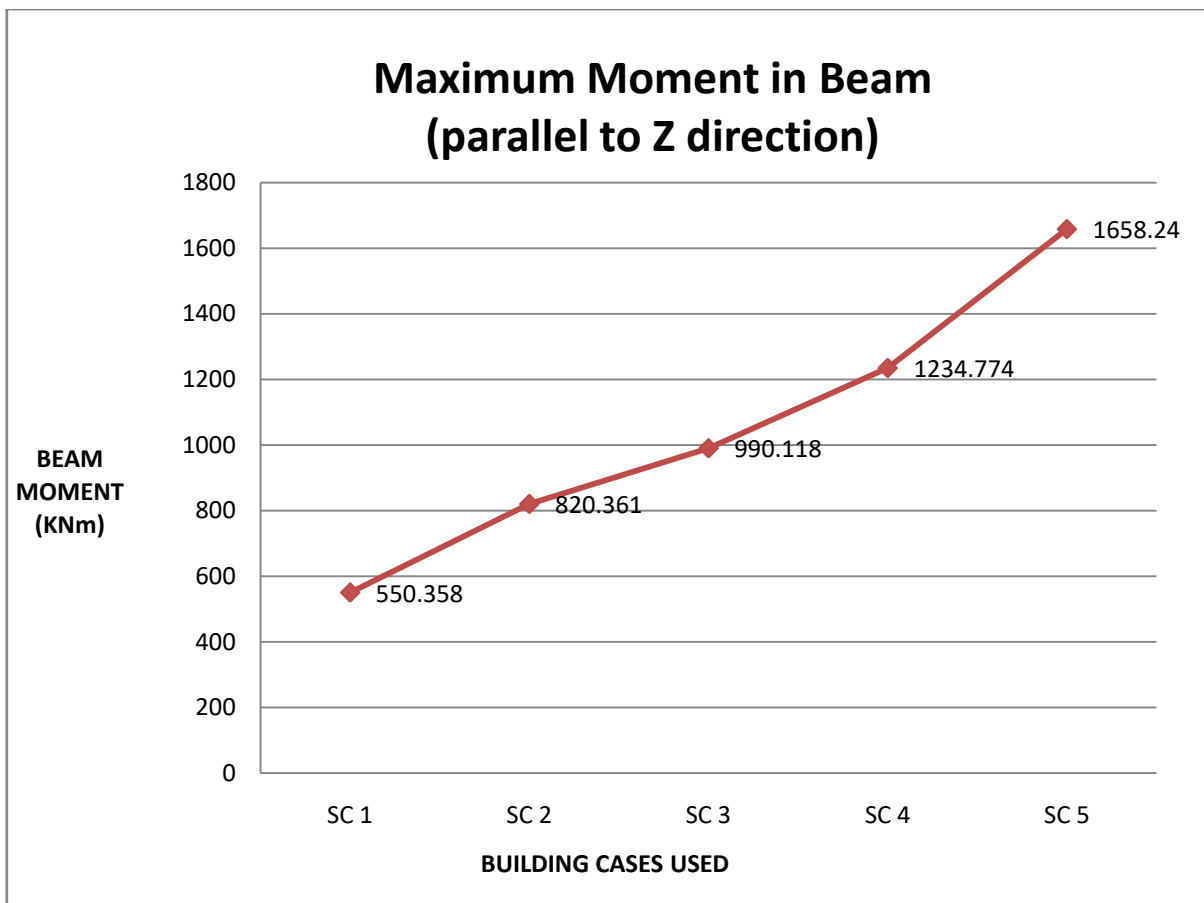


**Fig. 4.16:** Graphical Representation of Maximum Bending Moment in beams parallel to Z direction for all Single Core Cases

**Table 4.102:** Maximum Torsional Moment in beams along X and Z direction for all Single Core Cases

Single Core Case	Beam Torsional Moment (along X direction) (KNm)	Beam Torsional Moment (along Z direction) (KNm)
SC 1	26.523	22.015
SC 2	139.261	122.419
SC 3	121.953	106.396
SC 4	100.019	86.564
SC 5	89.625	77.265

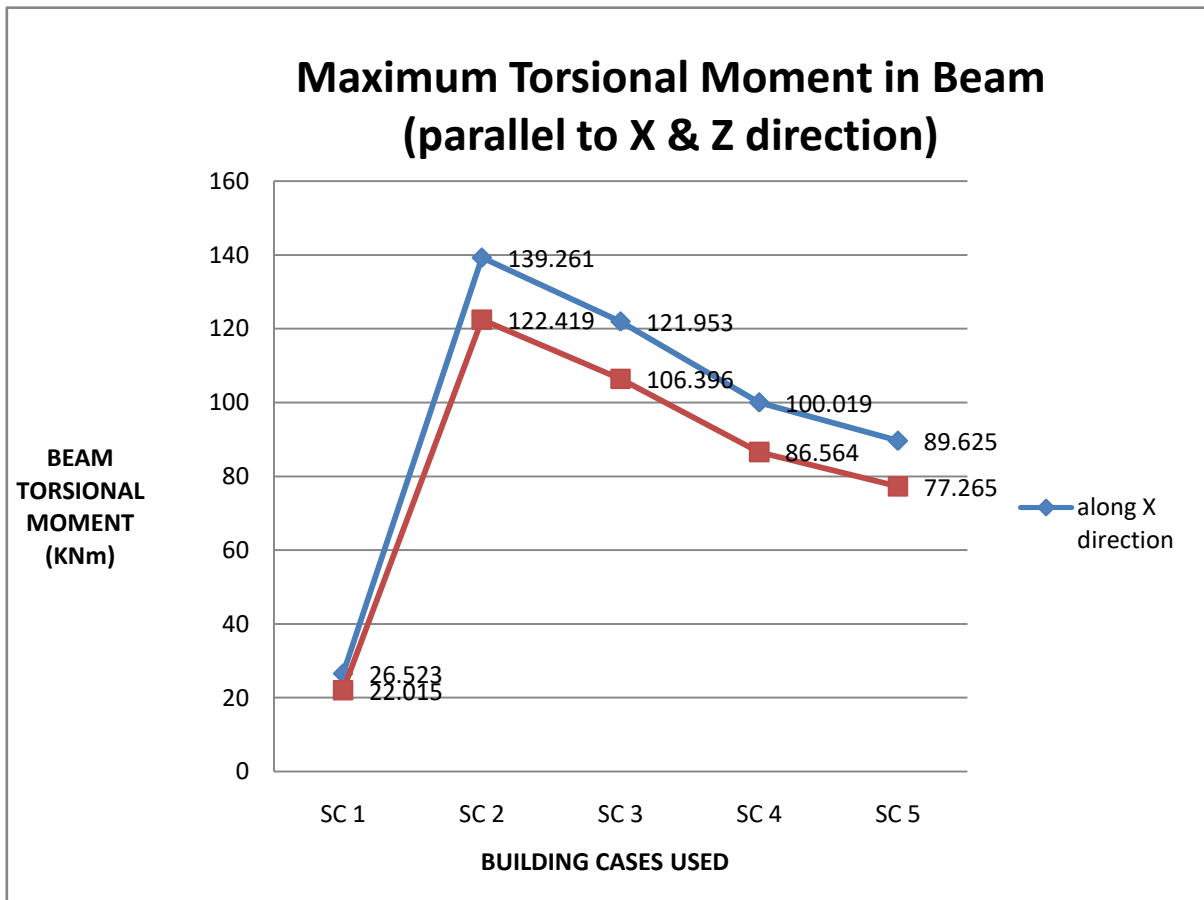


**Fig. 4.17:** Graphical Representation of Maximum Torsional Moment in beams along X and Z direction for all Single Core Cases

### 4.5 Discussions for Dual Core

**Table 4.103:** Maximum Displacement in X direction for all Dual Core Cases

Dual Core Case	Maximum Displacement (mm)
	For X Direction
DC 1	113.07
DC 2	124.23
DC 3	128.94
DC 4	131.78
DC 5	145.24
DC 6	221.99

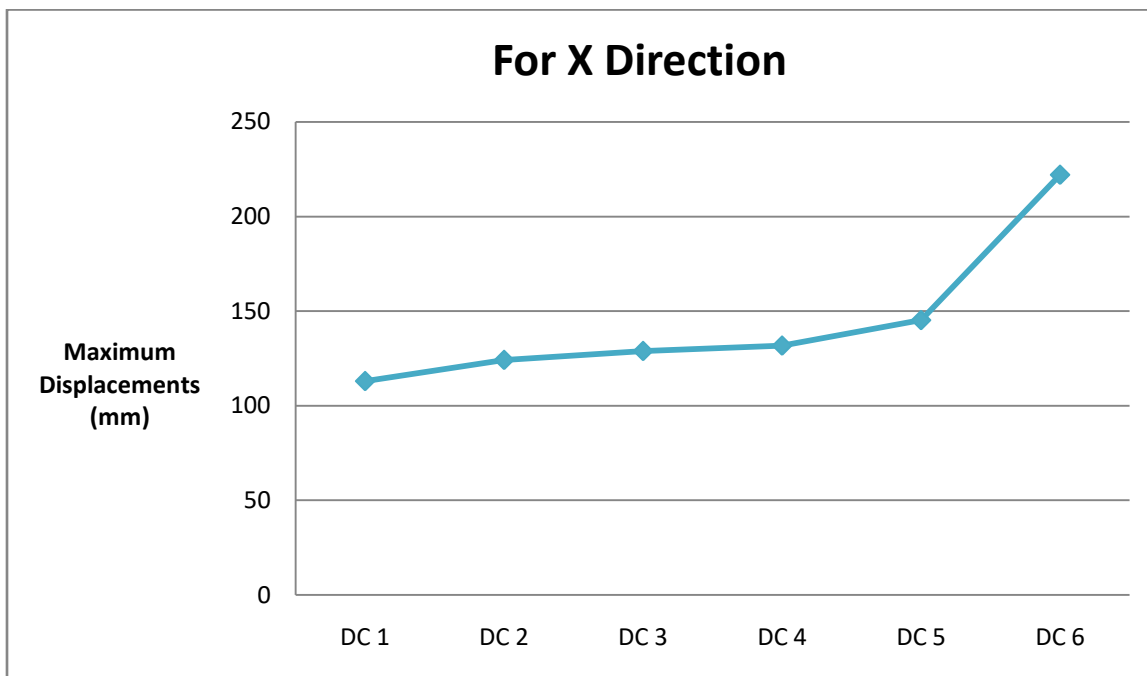


**Fig. 4.18:** Graphical Representation of Maximum Displacement in X direction for all Dual Core Cases



**Table 4.104:** Maximum Displacement in Z direction for all Dual Core Cases

Dual Core Case	Maximum Displacement (mm)
	For Z Direction
DC 1	213.7
DC 2	225.57
DC 3	228.06
DC 4	231.87
DC 5	244.47
DC 6	319.46

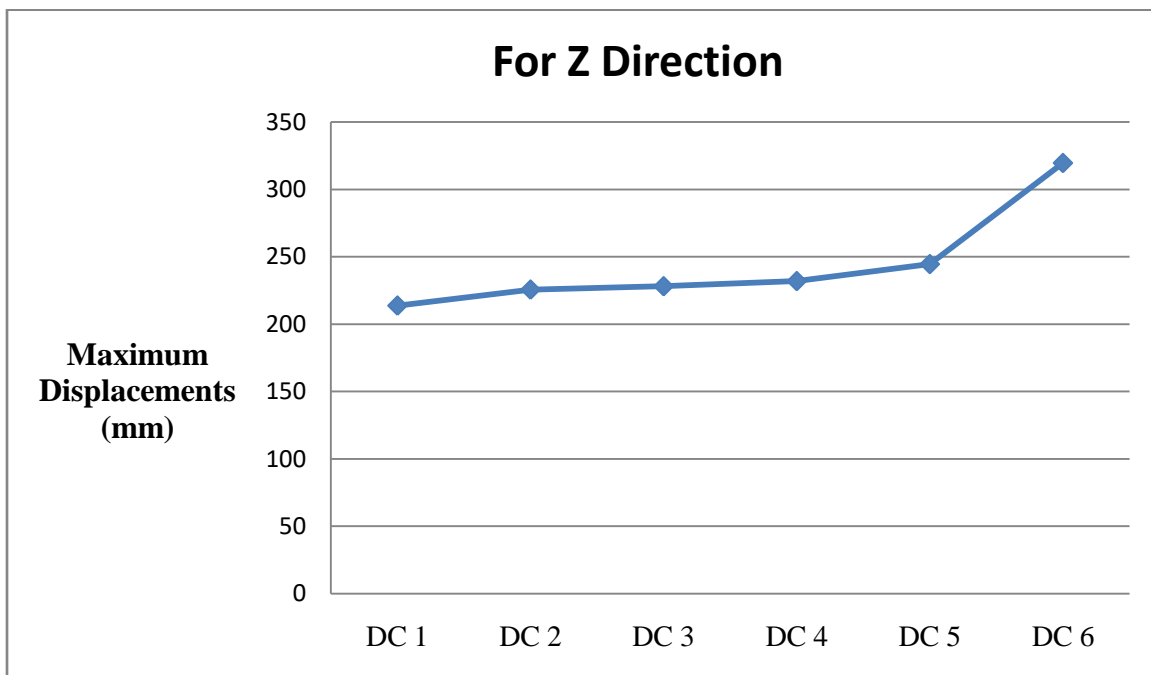


**Fig. 4.19:** Graphical Representation of Maximum Displacement in Z direction for all Dual Core Cases

**Table 4.105:** Storey Drift in X direction for all Dual Core Cases

S. No.	Height (m)	Storey Drift (cm)					
		For X Direction					
		DC 1	DC 2	DC 3	DC 4	DC 5	DC 6
1	0	0	0	0	0	0	0
2	3.5	0.1022	0.2057	0.2917	0.2961	0.4714	1.246
3	7	0.189	0.239	0.3454	0.375	0.5289	1.2702
4	10.5	0.2612	0.292	0.3804	0.4133	0.5343	1.1792
5	14	0.3268	0.3518	0.4335	0.4647	0.5735	1.1624
6	17.5	0.3841	0.4102	0.4828	0.5126	0.6122	1.1599
7	21	0.4338	0.4623	0.5265	0.5545	0.649	1.1619
8	24.5	0.4762	0.5088	0.5635	0.5902	0.6802	1.1635
9	28	0.5119	0.547	0.5946	0.6196	0.704	1.1618
10	31.5	0.5411	0.5786	0.6201	0.6428	0.7213	1.1551
11	35	0.5644	0.5784	0.6353	0.6601	0.7323	1.1422
12	38.5	0.582	0.6031	0.6524	0.6716	0.7378	1.1224
13	42	0.5944	0.6227	0.6603	0.6776	0.7383	1.0951
14	45.5	0.6019	0.637	0.6632	0.6783	0.7332	1.0599
15	49	0.6049	0.6481	0.6613	0.6741	0.7225	1.0164
16	52.5	0.604	0.643	0.655	0.6652	0.7064	0.9641
17	56	0.5996	0.6341	0.6449	0.6521	0.6853	0.903
18	59.5	0.5922	0.622	0.6313	0.6353	0.6595	0.8332
19	63	0.5826	0.6072	0.615	0.6152	0.6296	0.7553
20	66.5	0.5713	0.5906	0.5966	0.5928	0.5965	0.6709
21	70	0.5594	0.5731	0.5775	0.5692	0.5622	0.5856
22	73.5	0.5495	0.5559	0.5587	0.5466	0.5297	0.5065
23	77	0.5158	0.5318	0.5321	0.5162	0.4914	0.4348
24	80.5	0.5563	0.5574	0.561	0.5472	0.525	0.4522

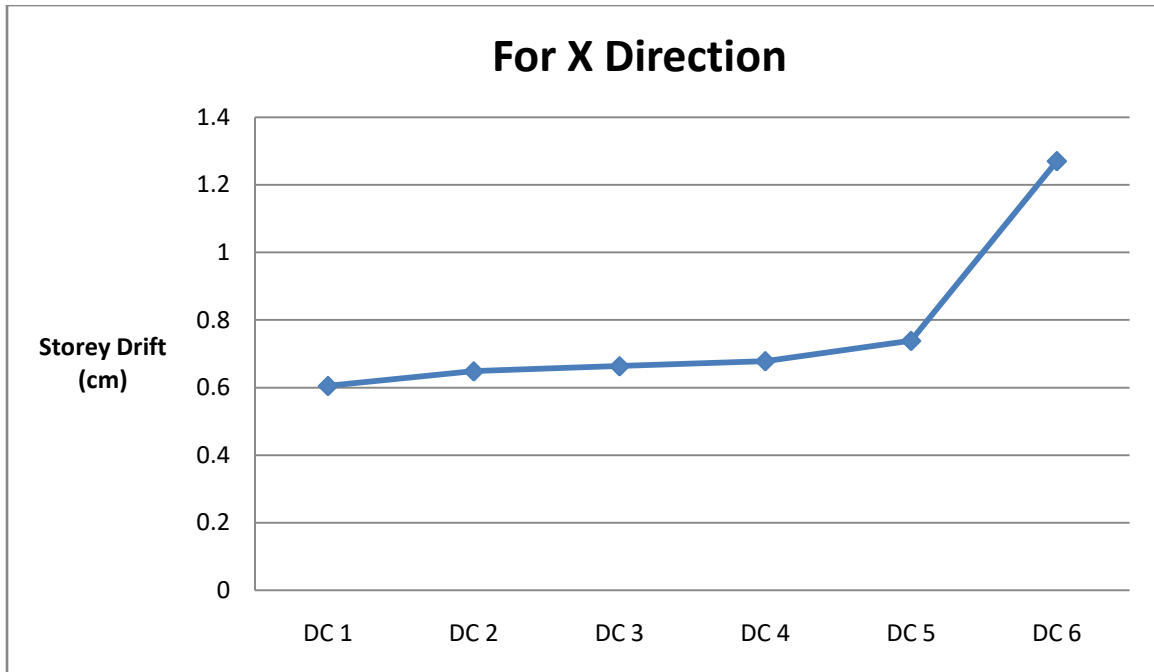


**Fig. 4.20:** Graphical Representation of Storey Drift in X direction for all Dual Core Cases

**Table 4.106:** Storey Drift in Z direction for all Dual Core Cases

S. No.	Height (m)	Storey Drift (cm)					
		For Z Direction					
		DC 1	DC 2	DC 3	DC 4	DC 5	DC 6
1	0	0	0	0	0	0	0
2	3.5	0.191	0.3203	0.3553	0.4262	0.6319	1.5465
3	7	0.3863	0.437	0.5754	0.634	0.8091	1.6526
4	10.5	0.5451	0.5438	0.7064	0.7508	0.8907	1.6178
5	14	0.6819	0.6789	0.8272	0.8635	0.9856	1.6353
6	17.5	0.7971	0.8021	0.1862	0.9559	1.0703	1.6557
7	21	0.8928	0.9037	1.0084	1.0341	1.1397	1.6736
8	24.5	0.971	0.9874	1.0732	1.0972	1.1927	1.6855
9	28	1.0332	1.0548	1.1241	1.1464	1.2319	1.6894
10	31.5	1.0807	1.1075	1.1602	1.1823	1.2585	1.684
11	35	1.1148	1.1071	1.1868	1.206	1.2733	1.6686
12	38.5	1.1367	1.1462	1.2002	1.2181	1.2782	1.6425
13	42	1.1473	1.173	1.2029	1.2194	1.2731	1.6051
14	45.5	1.1479	1.1879	1.1961	1.2107	1.2576	1.5559
15	49	1.1394	1.1719	1.1803	1.1926	1.2323	1.4943
16	52.5	1.123	1.1495	1.1563	1.166	1.1976	1.42
17	56	1.0999	1.1203	1.1253	1.1319	1.1543	1.3328
18	59.5	1.0717	1.0855	1.0883	1.0914	1.1033	1.2331
19	63	1.0398	1.0465	1.0469	1.0459	1.0457	1.1218
20	66.5	1.0062	1.0053	1.0029	0.9971	0.9837	1.0014
21	70	0.9732	0.9642	0.9589	0.948	0.9208	0.8787
22	73.5	0.9453	0.9263	0.9185	0.9029	0.8629	0.7656
23	77	0.8907	0.8865	0.8755	0.8554	0.8058	0.6672
24	80.5	0.9527	0.9265	0.9215	0.9070	0.8637	0.7024

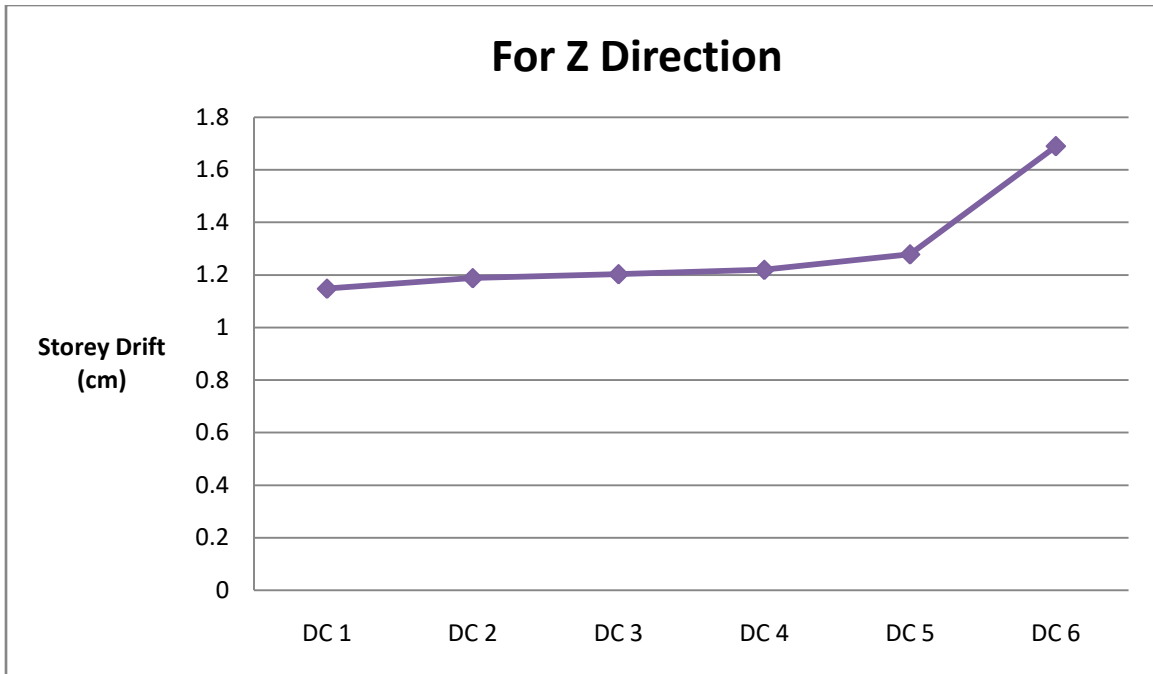


**Fig. 4.21:** Graphical Representation of Storey Drift in Z direction for all Dual Core Cases

**Table 4.107:** Base Shear in X and Z direction for all Dual Core Cases

Dual Core Case	Base Shear (KN)	
	X direction	Z direction
DC 1	6299.75	7268.48
DC 2	5760.62	6923.51
DC 3	5730.18	6828.63
DC 4	5719.54	6767.65
DC 5	5687.67	6731.39
DC 6	5596.22	6624.2

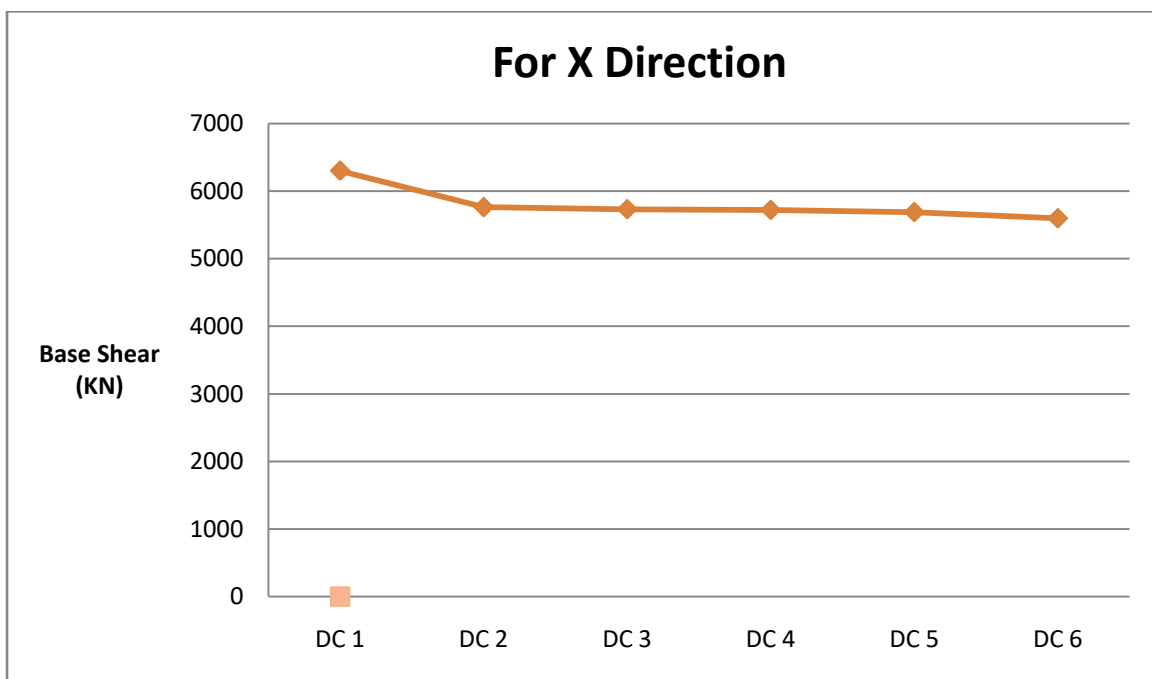


**Fig. 4.22:** Graphical Representation of Base Shear in X direction for all Dual Core Cases

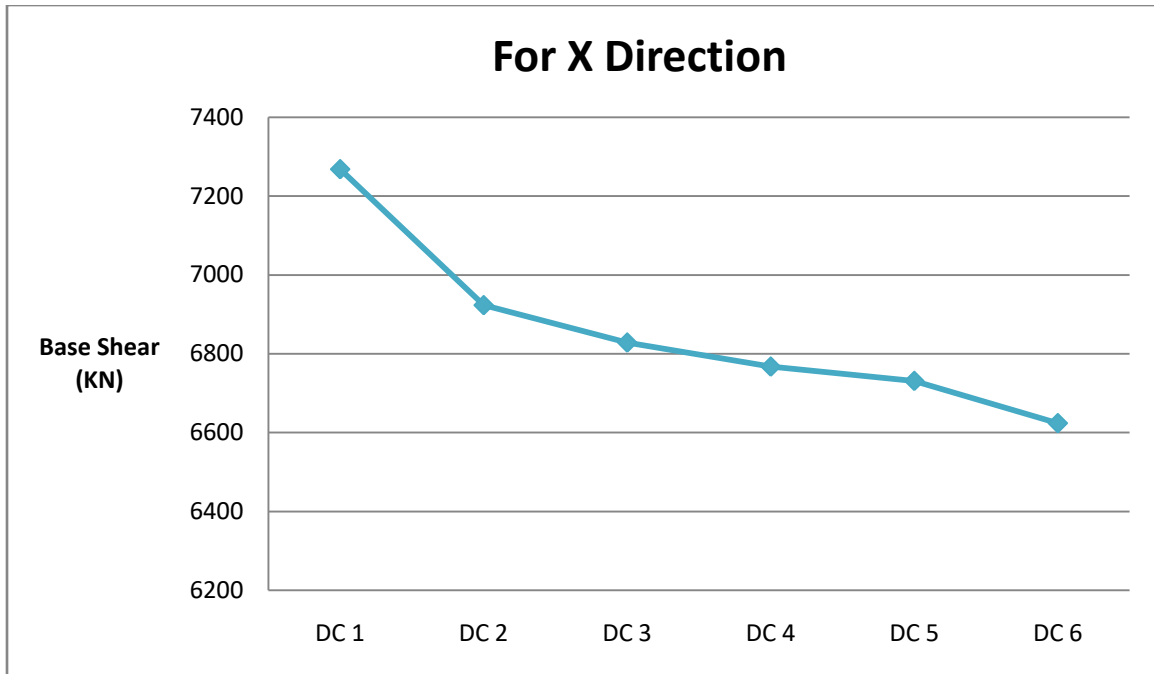


**Fig. 4.23:** Graphical Representation of Base Shear in X direction for all Dual Core Cases

**Table 4.108:** Time Period and Mass Participation Factor for all Dual Core Cases

Dual Core Case	Time Period (Seconds)	Participation X %	Time Period (Seconds)	Participation Z %
DC 1	2.688	67.678	3.451	69.153
DC 2	2.87	70.308	3.596	71.242
DC 3	2.915	71.011	3.626	71.653
DC 4	2.977	71.855	3.672	72.343
DC 5	3.175	74.195	3.818	72.252
DC 6	4.098	79.129	4.539	78.451

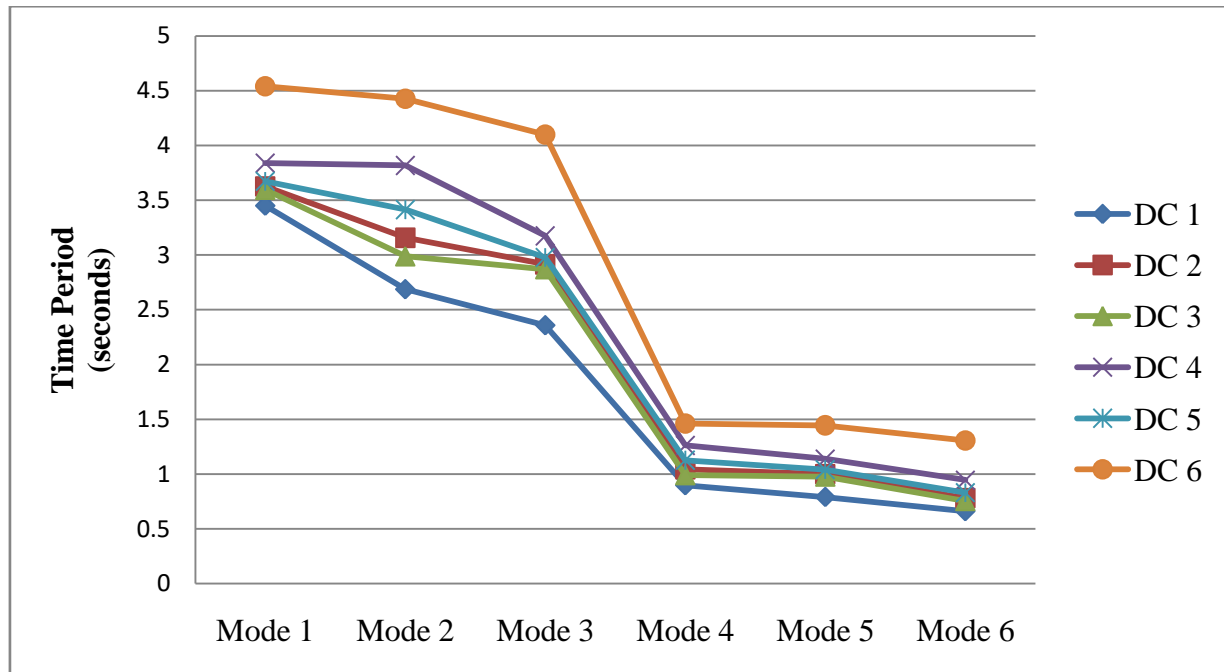


**Fig. 4.24:** Graphical Representation of Time Period Time Period for all Dual Core Cases



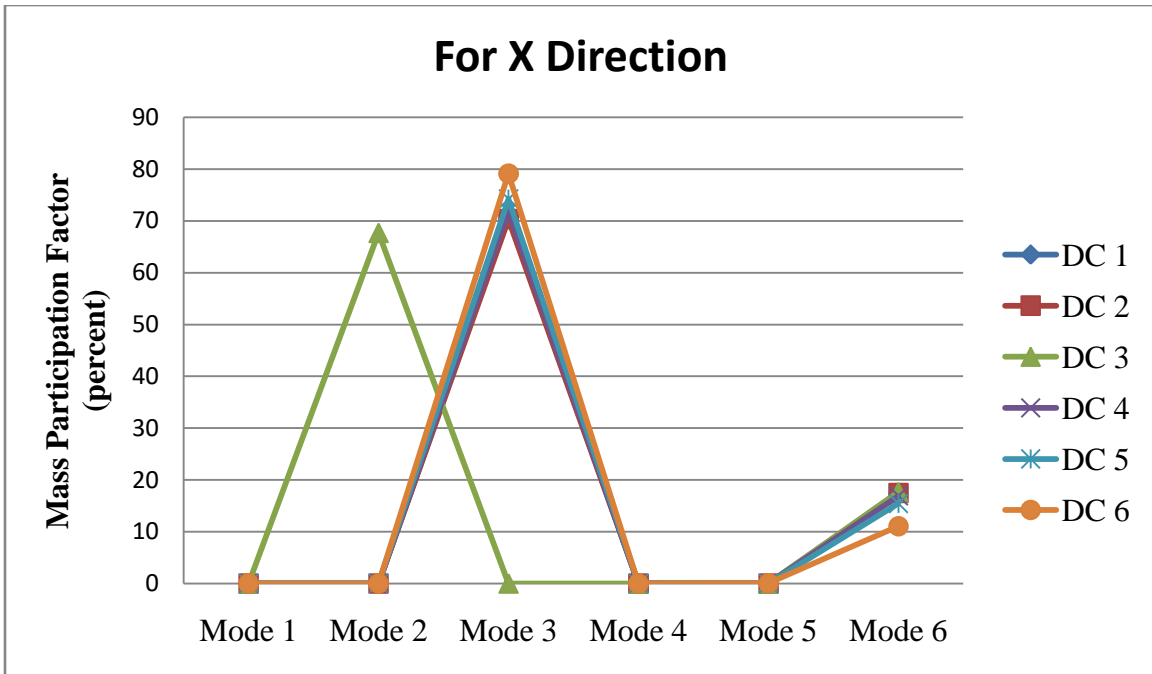


Fig. 4.25: Graphical Representation of Mass Participation Factor in X direction for all Dual Core Cases

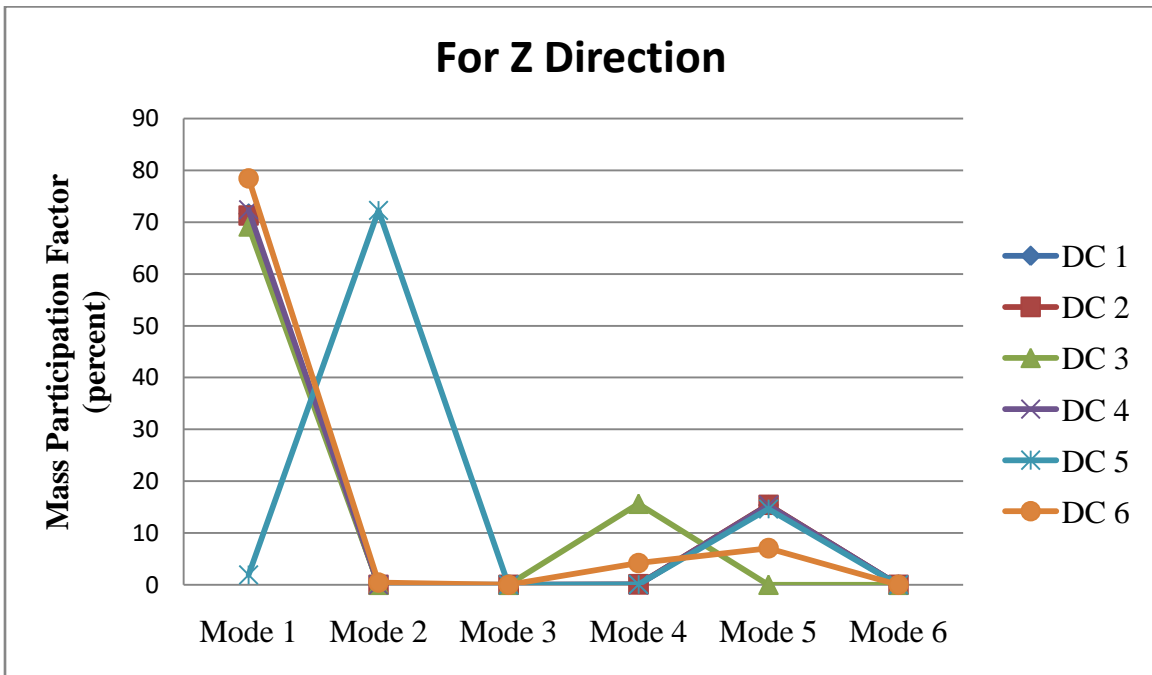
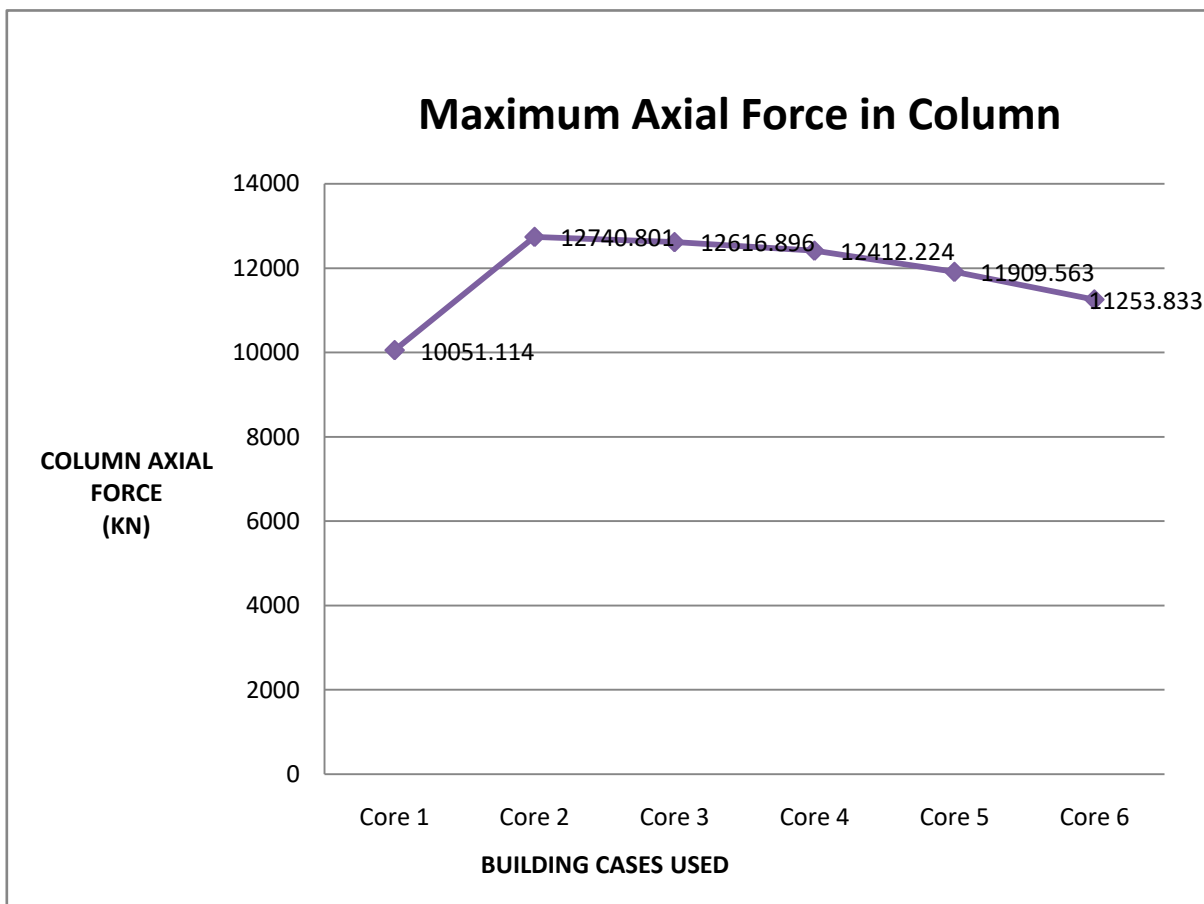


Fig. 4.26: Graphical Representation of Mass Participation Factor in Z direction for all Dual Core Cases

**Table 4.109:**Maximum Axial Forces in Column for all Dual Core Cases

Dual Core Case	Column Axial Force (KN)
DC 1	10051.114
DC 2	12740.801
DC 3	12616.896
DC 4	12412.224
DC 5	11909.563
DC 6	11253.833



**Fig. 4.27:** Graphical Representation of Maximum Axial Forces in Column for all Dual Core Cases

**Table 4.110:** Maximum Shear Forces in Columns for all Dual Core Cases

Dual Core Case	Column Shear Force (KN)	
	Shear along Y	Shear along Z
DC 1	304.381	337.489
DC 2	290.029	318.725
DC 3	287.137	314.48
DC 4	279.713	307.252
DC 5	262.364	293.618
DC 6	513.489	429.797

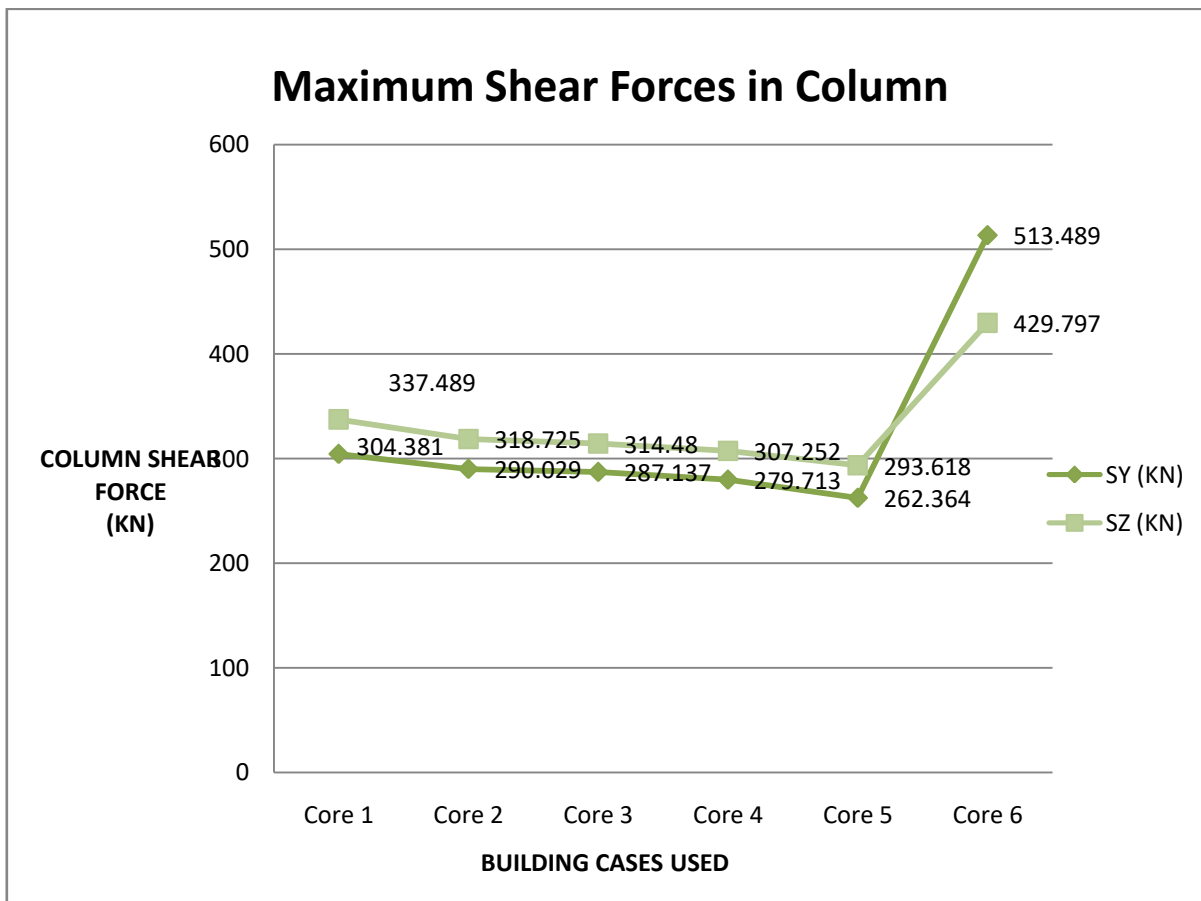


**Fig. 4.28:** Graphical Representation of Maximum Shear Forces in Columns for all Dual Core Cases

**Table 4.111:** Maximum Bending Moment in Columns for all Dual Core Cases

Dual Core Case	Column Bending Moment (KNm)	
	Moment along Y	Moment along Z
DC 1	653.345	600.995
DC 2	617.427	573.181
DC 3	609.354	567.603
DC 4	595.567	553.19
DC 5	559.416	519.482
DC 6	844.657	988.533

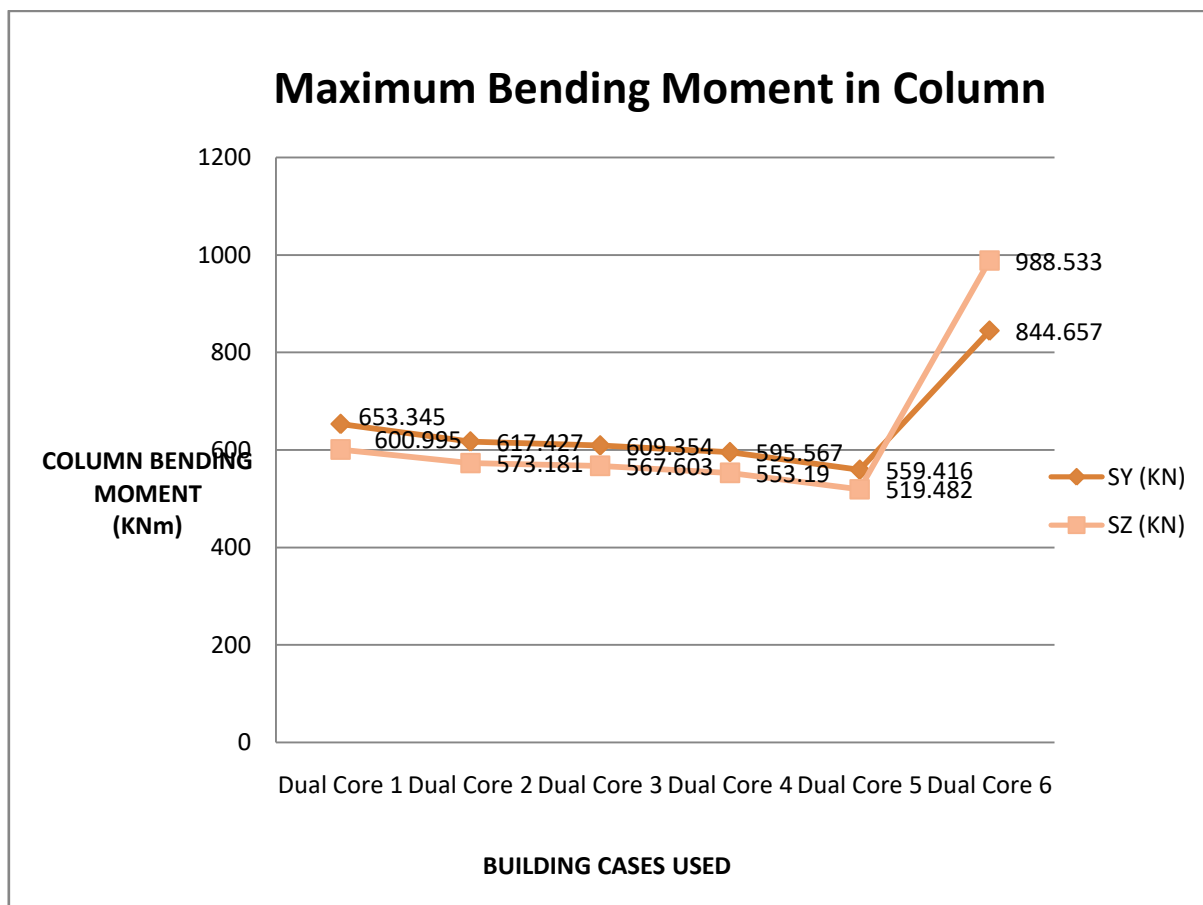


**Fig. 4.29:** Graphical Representation of Maximum Bending Moment in Columns for all Dual Core Cases

**Table 4.112:** Maximum Shear Forces in beams parallel to X direction for all Dual Core Cases

Dual Core Case	Beam Shear Force (parallel to X direction) (KN)
DC 1	247.888
DC 2	2026.618
DC 3	3214.451
DC 4	2107.112
DC 5	2035.917
DC 6	726.348

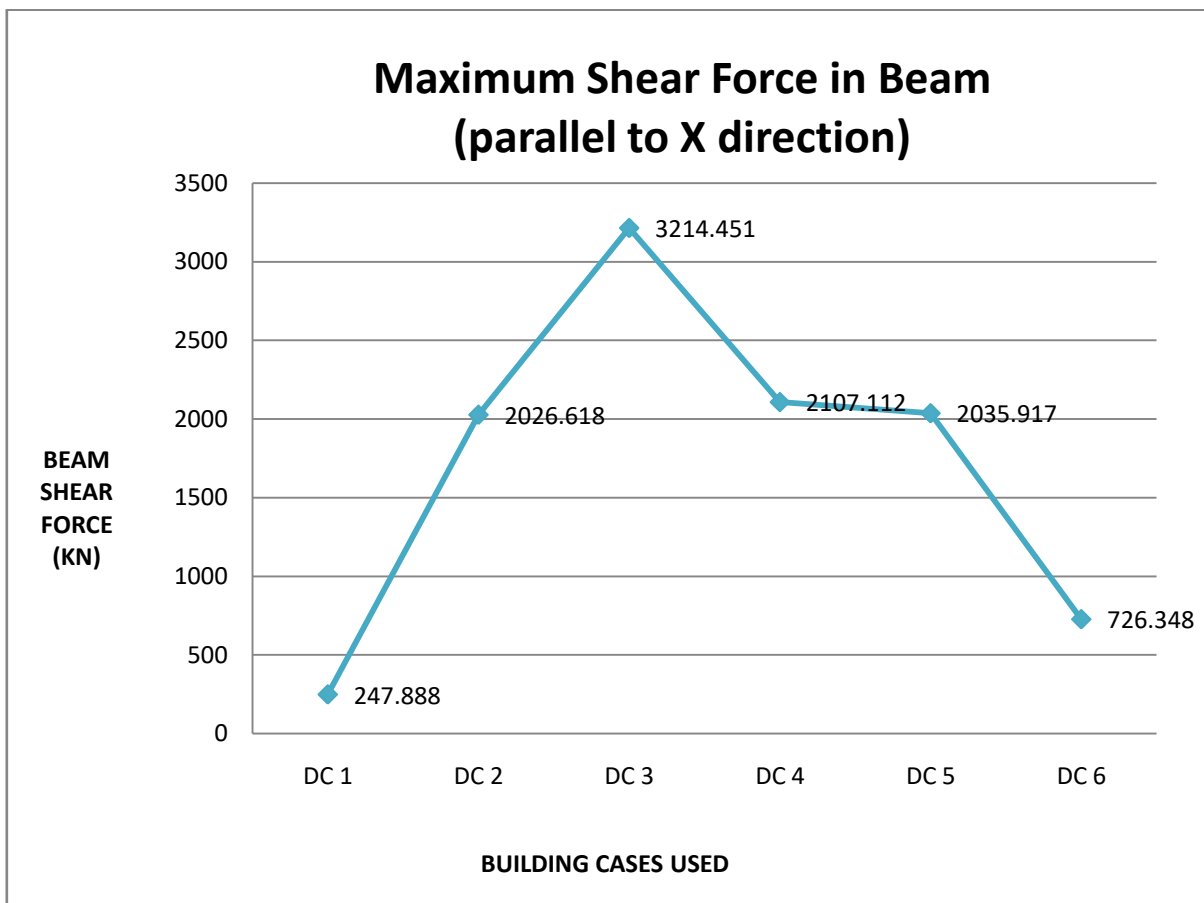


**Fig. 4.30:** Graphical Representation of Maximum Shear Forces in beams parallel to X direction for all Dual Core Cases

**Table 4.113:** Maximum Shear Forces in beams parallel to Z direction for all Dual Core Cases

Dual Core Case	Beam Shear Force (parallel to Z direction) (KN)
DC 1	259.414
DC 2	2268.144
DC 3	2369.9
DC 4	2399.369
DC 5	2358.449
DC 6	802.527

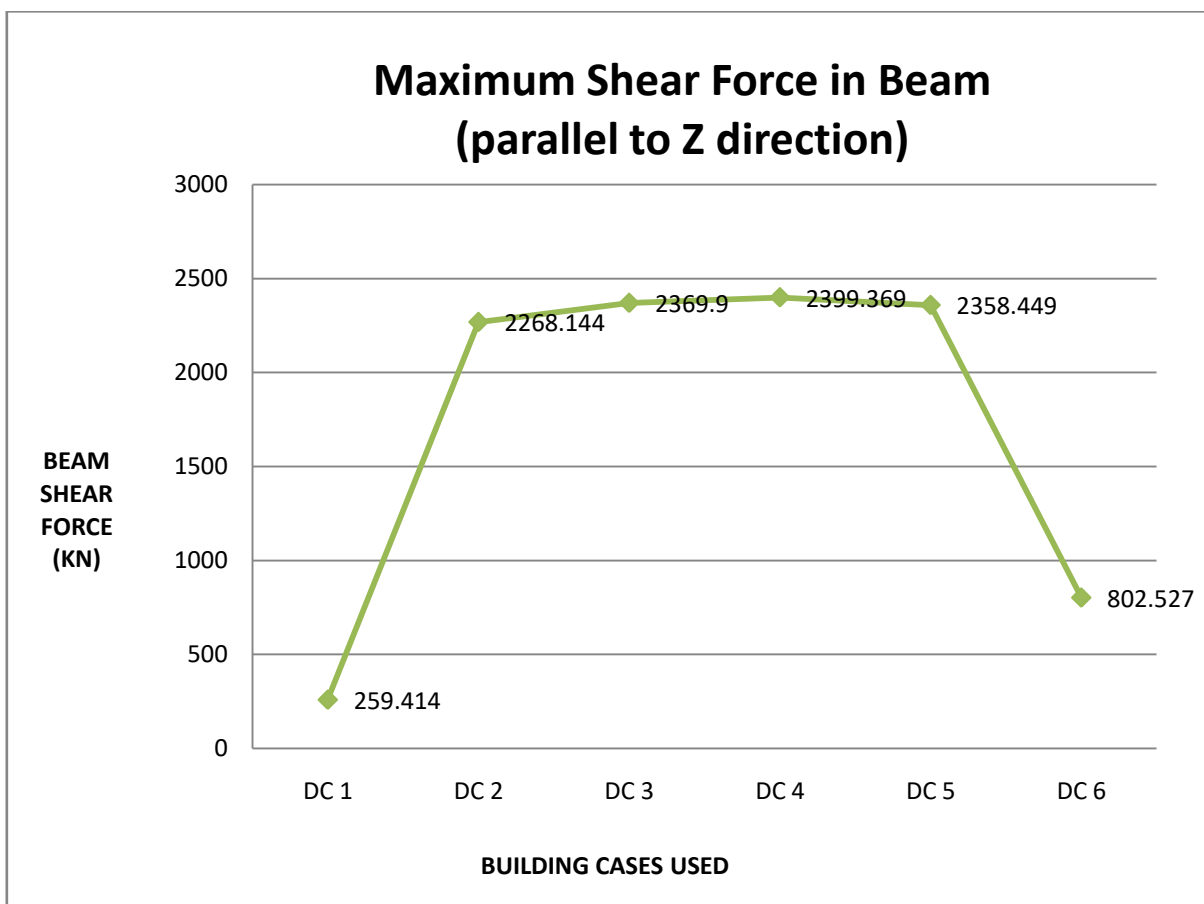


**Fig. 4.31:** Graphical Representation of Maximum Shear Forces in beams parallel to Z direction for all Dual Core Cases

**Table 4.114:** Maximum Bending Moment in beams parallel to X direction for all Dual Core Cases

Dual Core Case	Beam Bending Moment (along X direction) (KNm)
DC 1	491.692
DC 2	604.596
DC 3	1015.64
DC 4	879.871
DC 5	1313.06
DC 6	923.411

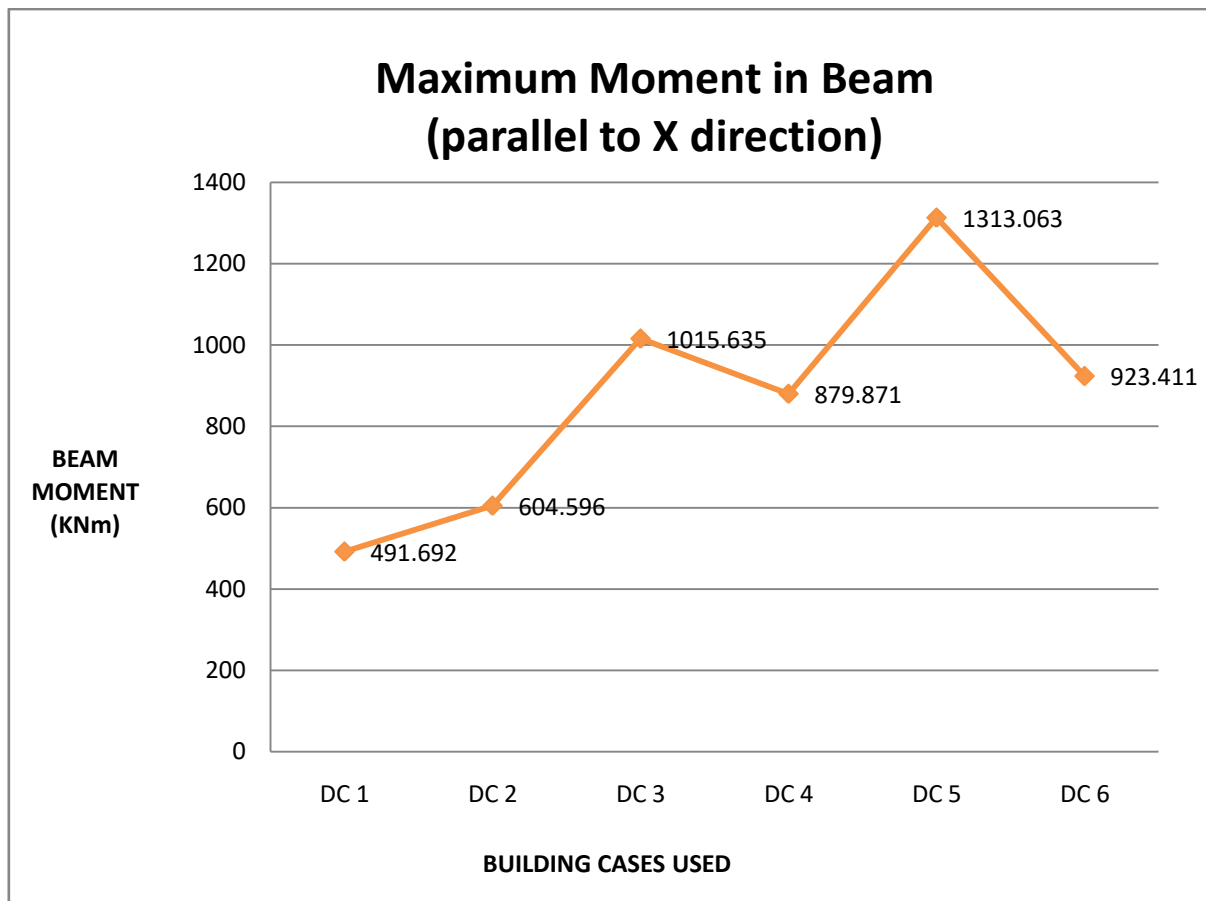


**Fig. 4.32:** Graphical Representation of Maximum Bending Moment in beams parallel to X direction for all Dual Core Cases

**Table 4.115:** Maximum Bending Moment in beams parallel to Z direction for all Dual Core Cases

Dual Core Case	Beam Bending Moment (along Z direction) (KNm)
DC 1	541.083
DC 2	627.5
DC 3	707.573
DC 4	1018.64
DC 5	1494.85
DC 6	1020.58

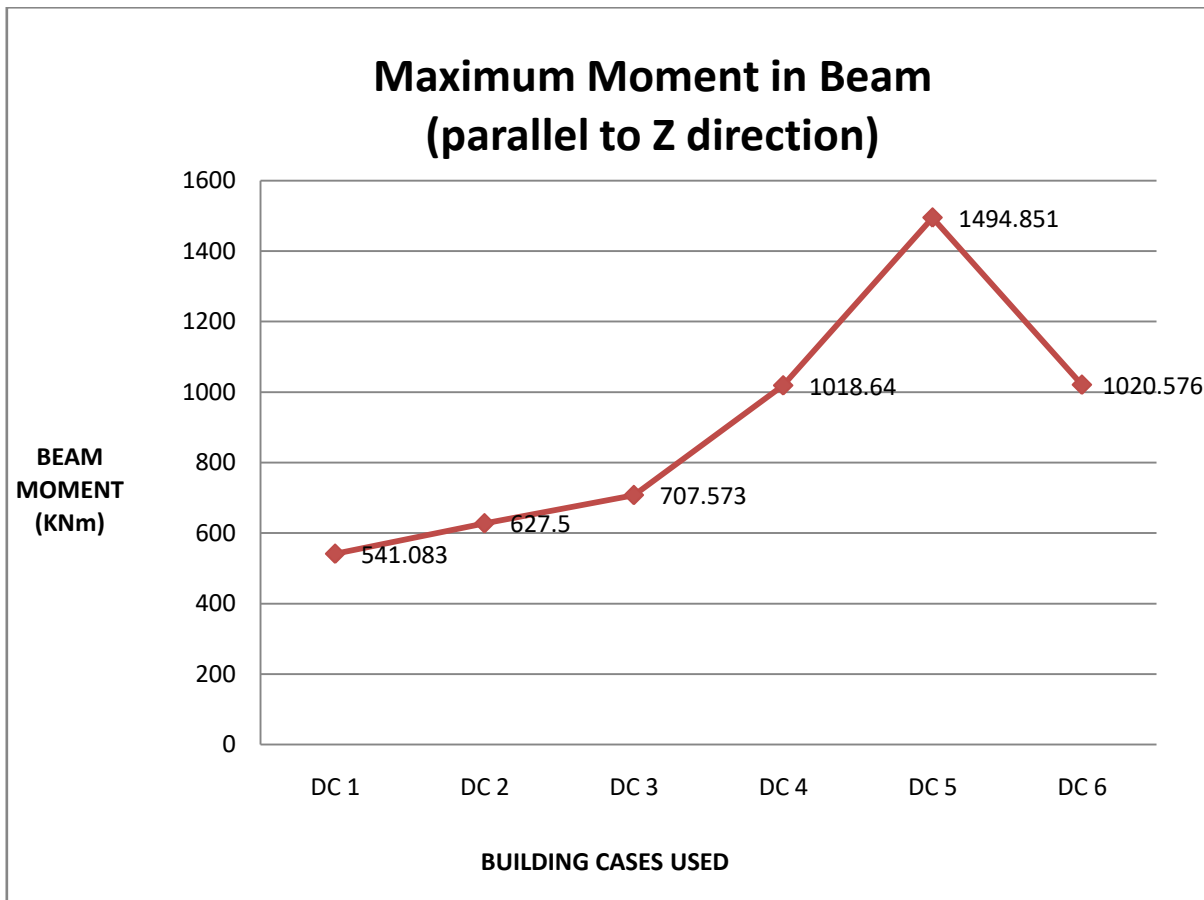


**Fig. 4.33:** Graphical Representation of Maximum Bending Moment in beams parallel to Z direction for all Dual Core Cases



**Table 4.116:** Maximum Torsional Moment in beams along X and Z direction for all Dual Core Cases

Dual Core Case	Beam Torsional Moment (along X direction) (KNm)	Beam Torsional Moment (along Z direction) (KNm)
DC 1	28.755	24.145
DC 2	135.109	103.916
DC 3	118.255	90.254
DC 4	97.073	73.424
DC 5	82.594	62.799
DC 6	99.438	73.582

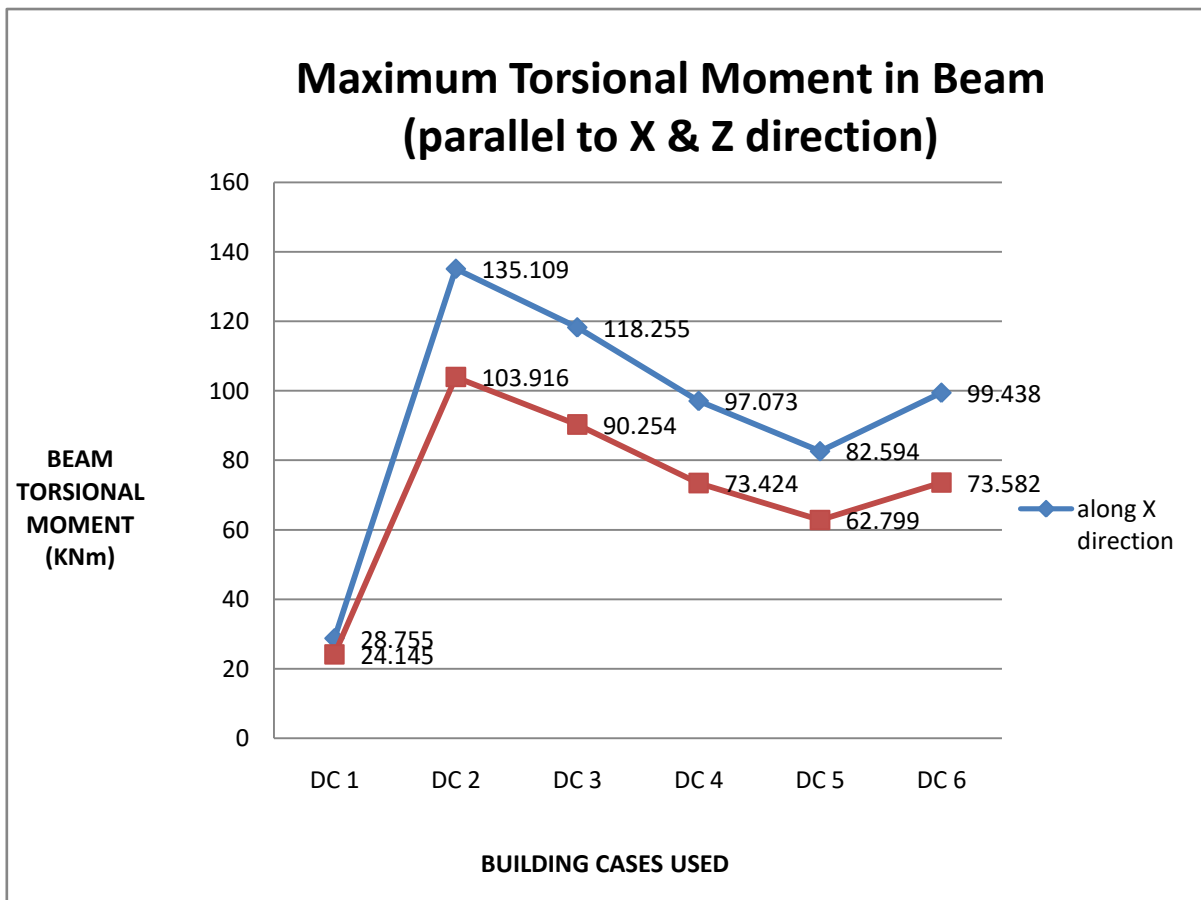


**Fig. 4.34:** Graphical Representation of Maximum Torsional Moment in beams along X and Z direction for all Dual Core Cases

### III. CONCLUSION

Analysis of five different single and dual-core building instances reveals various outcomes for each structure. The comparison study yields the following conclusions for single-core buildings:

The maximum displacement in both the X and Z directions increases when the shear wall area is reduced. Furthermore, when the opening area exceeds 10%, the displacements for single-core examples also increase.

Storey drift responds similarly to displacement in both the X and Z directions. As the shear wall area decreases in single-core situations, the floor drift increases.

Base shear values decrease with an increase in the opening area percentage, as the structure's weight rises. Building SC 5 demonstrates the best parametric values with a 25% shear wall opening in both the X and Z directions.

The time span for both lateral and transitional seismic effects should not exceed 3.5 seconds. SC 5 proves to be the most effective at limiting the parametric values among all the buildings.

The mass participation of the comparison is within the allowed range according to Indian Standardization. Building SC 5 is the greatest option for limiting the parametric values.

Building SC 5 is the most cost-effective among all options due to the values of Maximum Axial Forces in columns, increasing from 0% to 10% opening area, and then steadily decreasing.

Erecting SC 5 is the most cost-effective option because shear forces in columns in both the Y and Z axes continuously decrease as the area of the shear wall aperture increases.

Maximum Bending Moment values decrease in the column from core case 1 to SC 5, making SC 5 the most affordable among all options in this criterion.

In multi-story structures, reducing the area used by the shear wall results in drastic values in both the longitudinal and transverse direction beams. These values initially rise before continuing to fall. The cost of building SC 5 is the lowest among all options.

The values of moments in the beam, both in the X and Z directions, progressively rise until they reach the limit value of building SC 5. After that, the beam collapses. This holds true for moments in the beam.

Torsion in the beam displays the limiting parametric values up to constructing SC 5 when the shear wall area is reduced.

For single-core structures, building SC 5 exhibits the best parametric values among all options, particularly in handling seismic effects

## 5.2 Conclusion for Dual Core:

The study of dual-core buildings yields the following conclusions:

Reduction in shear wall area leads to increased maximum displacement in both the X and Z directions. In dual-core scenarios, displacement also increases when the opening exceeds 10%.

Storey drift responds similarly to displacement in both the X and Z directions, with the floor drift increasing as the shear wall area decreases in dual-core situations.

Base shear values decrease as the opening area percentage rises and the structure's weight decreases. Building DC 6 demonstrates the best parametric values with a 50% shear wall opening in both the X and Z axes.

The time period for both lateral and transitional seismic effects should not exceed 3.5 seconds. DC 6 proves to be the most effective at limiting the parametric values among all the buildings.

Mass participation in the comparison aligns with Indian Standardization, and Building DC 6 exhibits the best limitation of parametric values.

Building DC 6 is the most cost-effective option among all with a 50% opening area, as the values of the maximum axial forces in the column initially increase from 0% to 10% opening area and then steadily decrease.

With an increase in the shear wall opening area, shear forces in the column in both the Y and Z axes continuously decrease. DC 5 is the most cost-effective among all options.

Maximum Bending Moment values in the column decrease from DC 1 to DC 5, making DC 5 the most affordable option in this criterion.

Shocking values in longitudinal direction beams are observed due to the multi-story building's reduced use of the shear wall. DC 3 and DC 6 show peak values, with the lowest percentage loss in wall area observed in DC 3.

The values in transverse direction beams are affected by the reduction in the area used by shear walls in multi-story structures. Dual core case 6 exhibits the best parametric value, while the peak value is seen in dual core case 5.

Fluctuating values in moments in beams indicate that shear force gradually increases beyond the limit. It appears that under building DC 5, structural components are safe in moments, and beyond this, the beam fails. This applies to moments in beams in both the X and Z directions.

Torsion in the beam exhibits limiting parametric values under DC 2 when there is a deduction in the shear wall area.

Building DC 6 exhibits the best seismic effects among dual core buildings.

## REFERENCES

- [1] C. Marthong, T. P. Agrawal, "Effect of Fly Ash Additive on Concrete Properties" International Journal of Engineering Research and Applications July-August 2012.
- [2] Markanday Giri, Sagar Jamle and Kundan Meshram (2020), "Response Spectrum Analysis", LAP LAMBERT Academic Publishing, Mauritius.
- [3] Ms. Priyanka Sonil, Mr. Purushottam Lal Tamrakar, Vikky Kumhar, (2016), "Structural Analysis of Multistory Building of Different Shear Walls Location and Heights" International Journal of Engineering Trends and Technology (IJETT) – Vol. 32, No. 1.

- [4] N. Anand, G. Prince Arulraj, "Effect of Grade of Concrete on the Performance of Self-Compacting Concrete Beams Subjected to Elevated Temperatures" *Fire Technology*, 50, 1269–1284, 2014 Springer Science + Business Media New York. DOI: 10.1007/10694-013-0345–6.
- [5] Prabhulal Chouhan, Sagar Jamle, M.P. Verma, (2017), "Experimental Investigation On Silica Fume As Partial Replacement Of Cement For M-25 Grade Concrete", *IJSART - Volume 3 Issue 5*, ISSN- 2395-1052.
- [6] Prakash Mandiwal, Sagar Jamle, (2018), "Use of Polyethylene Glycol as Self Curing Agent in Self Curing Concrete - An Experimental Approach", *International Research Journal of Engineering and Technology*, (ISSN:2395-0072(P), 2395-0056(O)), vol. 5, no. 11, pp. 916-918.
- [7] Sachin Sironiya, Sagar Jamle, M. P. Verma, (2017), "Experimental Investigation On Fly Ash & Glass Powder As Partial Replacement Of Cement For M-25 Grade Concrete", *IJSART - Volume 3 Issue 5*, ISSN- 2395-1052, pp. 322-324.
- [8] Sagar Jamle, Dr. M.P. Verma, Vinay Dhakad, (2017), "Flat Slab Shear Wall Interaction for Multistoried Building under Seismic Forces", *International Journal of Software & Hardware Research in Engineering (IJSHRE)* ISSN: 2347-4890 Vol.-05, Issue-3, pp. 14-31.
- [9] Sameer Khan, Sagar Jamle, M.P. Verma, (2017), "Experimental Investigation with Marble Dust Powder as a Partial Swap of Cement for M 20 Grade Concrete", *IJSART- Volume 3 Issue 6*, ISSN- 2395-1052, pp. 256-259.
- [10] Shankar H. Sanni, R. B. Khadiranaikar, (2013), "Performance of Alkaline Solutions on Grades of Geopolymer Concrete", *IJRET: International Journal of Research in Engineering and Technology*.
- [11] Tiwari Darshita, Patel Anoop, (2014), "Study of Strength and Workability of Different Grades of Concrete by Partial Replacement of Fine Aggregate by Crushed Brick and Recycled Glass Powder", *International Journal of Science and Research (IJSR)*.
- [12] Wensheng LU, Xilin LU, (1998), "Seismic Model Test and Analysis of Multi - Tower High-Rise Buildings" *Research Institute of Engineering Structures, Tongji University, Shanghai, P. R. China*.
- [13] Apurva Joshi, Ankit Pal . (2020) Determination of Performance point of stability improvement of the multistoried building using different grade of concrete in beams at different levels over soft soil *Journal of Xi'an University of Architecture & Technology*, Volume XII, Issue IX, 2020 <https://doi.org/10.37896/JXAT12.09/2858> ISSN No. : 1006-7930 pp 92-103
- [14] Joshi A. , Pal A. , Vishwakarma A. (2020) Determination of Performance Point of Stability Improvement of the Multistoried Building using Different Grade of Concrete in Beams at Different Levels over Soft Soil: A Review *International Journal of Advanced Engineering Research and Science* Vol-7, Issue-8, DOI: <https://dx.doi.org/10.22161/ijaers.78.25>, ISSN: 2349-6495(P) 2456-1908(O) pp 241-246
- [15] Sunil Rathore, Ankit Pal, Arvind Vishwakarma. (2020). Accumulative Stability Increment of Multi-Storeyed Building Rested Over Soft, Medium and Hard Soil: A Review *International Journal of Advanced Engineering Research and Science (IJAERS)*, Vol.7, issue 7, <https://dx.doi.org/10.22161/ijaers.77.50>, ISSN: 2349-6495(P) | 2456-1908(O) pp 442-448
- [16] Sunil Rathore. , Ankit Pal , Arvind Vishwakarma. (2020) Accumulative Stability Increment of Multi-Storeyed Building Rested over Soft, Medium and Hard Soil using Different Grades of Concrete in Beam *Journal of Xi'an University of Architecture & Technology*, Volume XII, Issue VIII, 2020 <https://doi.org/10.37896/JXAT12.08/2627> ISSN No. : 1006-7930 pp 260-277